A DISSERTATION FOR THE DEGREE OF DOCTOR OF PHILOSOPHY

# Development of Photosynthesis and Growth Models of Sweet Basil and Ice Plant in Plant Factories

# 식물공장 재배 바질과 아이스플랜트의 광합성 및 생육 모델 개발


BY

KYOUNG SUB PARK


FEBRUARY, 2016


MAJOR IN HORTICULTURAL SCIENCE

DEPARTMENT OF PLANT SCIENCE

THE GRADUATE SCHOOL OF SEOUL NATIONAL UNIVERSITY

# Development of Photosynthesis and Growth Models of Sweet Basil and Ice Plant in Plant Factories

Kyoung Sub Park

Department of Plant Science

The Graduate School of Seoul National University

## ABSTRACT

The objective of this study was to develop photosynthesis and growth models of sweet basil and ice plant under plant factory environments. For photosynthesis, biochemical models coupled with stomatal conductance and transpiration were considered. Saturation and compensation points of both plants for light and $CO_2$ were determined by regression analyses of light and $CO_2$ response curves, respectively. In the photosynthesis of sweet basil, non-rectangular hyperbola was the most suitable for The saturation and compensation points for light and $CO_2$ were determined as 545.3, 26.5,

728.8 and 85.05 μmol·m$^{-2}$·s$^{-1}$, respectively, by the modified non-rectangular hyperbola model. The maximum carboxylation rate, potential rate of electron transport, and rate of triose phosphate utilization calculated by Sharkey's regression were 102.6, 117.7, and 7.41 μmol·m$^{-2}$·s$^{-1}$, respectively. The results showed that the coupled biochemical model was effective for predicting the photosynthesis of sweet basil leaves comparing to other descriptive models. For ice plant under plant factory environments, the saturation and compensation points for light and $CO_2$ were 569.5, 56.02, 632.9, and 117.2 μmol·m$^{-2}$·s$^{-1}$, respectively. The maximum carboxylation rate, potential rate of electron transport, and rate of triose phosphate utilization were calculated as 222.3, 234.9, and 13.0 μmol·mol$^{-1}$, respectively. The parameters of minimum stomatal conductance of water vapor at the light compensation point and empirical coefficient in the BWB model could be solved as 0.0487and 0.0012, respectively. Finally, the growth models for temperature and $CO_2$ concentration were developed by using an expo-linear model. Adequate air temperature and $CO_2$ concentration for sweet basil and ice plant were 25$^{o}$C and 800 μmol·mol$^{-1}$, respectively. From this study, the coupled biochemical model was more effective for explaining the photosynthesis of sweet basil and ice plant during the juvenile stage under plant factory conditions.

*Keywords:* coupled model, FvCB model, growth model, ice plant, photosynthesis model, sweet basil

Student Number: 2003-30360

## CONTENTS

# LIST OF TABLES

## LIST OF FIGURES

## LIST OF ABBREVIATIONS

$A$, net photosynthesis rate

$A_c$, rubisco-limited photosynthetic rate

$A_j$, RuBP regeneration limited photosynthetic rate through electron transport

$A_p$, TPU limited photosynthetic rate

$A_{max}$, maximum net photosynthesis rate

$C_a$, ambient $CO_2$ concentration

$C_c$, chlloroplastic $CO_2$ concentration

$C_i$, intercellular $CO_2$ concentration

$C_s$, leaf surface $CO_2$ concentration

$E$, transpiration rate

$g_m$, mesophyll conductance

$g_s$, stomatal conductance

$h_s$, relative humidity at the leaf surface

$I$, photosynthetically active photon flux

$J$, electron transport rate (=ETR)

$J'$, rate of carboxylation allowed by the electron transport

$K_c$, Michaelis constant for $CO_2$

$K_o$, Michaelis constant for $O_2$

$k_c$, turnover rate constant for $CO_2$

$k_o$, turnover rate constant for $O_2$

PPFD, photosynthetic photon flux density

$P_r$, photorespiration

$R_d$, mitochondrial respiration in the light or dark respiration

$V_c$, velocity of carboxylation

$V_{cmax}$, maximum velocity of carboxylation

$V_o$, velocity of oxygenation

$V_{omax}$, maximum velocity of oxygenation

WUE, water use efficiency, $A_n/E$

$\alpha$, apparent quantum yield

$\alpha$, carboxylation efficiency

$\theta$, curvature of curve

$\Gamma_{light}$, light compensation point

$\Gamma$, $CO_2$ compensation point

$\Gamma_*$, $CO_2$ compensation point in the absence of $R_d$

# INTRODUCTION

Plant factories are closed-type growing systems for continuous and sustainable crop production and in most cases independent of outdoor environmental conditions. The key concept of the closed-type plant factory is year-round and planned crop productions with high yield and quality through the accurate environment controls. According to Kozai (2007, 2013) and Goto (2012), highly-developed plant factory systems usually have following principle components: a thermally insulated, airtight container or warehouse-type closed structure, hydroponic growing beds which are arranged in a vertically stacked layers within cultivation area, artificial lighting system which can be designed using fluorescent and/or LED (light emitting diodes) lamps, $CO_2$ supply unit, air conditioning as well as heating sys-

tem. An absence of insects and plant diseases due to closed and sterile environments and consequently zero application of pesticides will ensure production of safe, healthy and fresh vegetables.

A wide variety of crops can be grown in plant factories including leaf vegetables and medicinal herbs. However crops for the commercial production should have characteristics of high functionality, fast growth, and rapid consumption due to marketing trends. Also plants must have relatively short and compact canopy to be able to grow normally in a short distance between growing beds.

Sweet basil (*Ocimum basilicum* L.) and common ice plant (*Mesembryanthemum crystallinum* L.) are considered as proper crops with high commercial potential for the production in closed-type plant factories owing to their

unique taste and high prices comparable with fresh ginseng prices, which is also very important point considering high production and operation costs in plant factories. Their utilization and consumption are becoming very extensive as a high functional-food, spice and medicinal herb and consumer demand for such crops will undoubtedly increase.

For wider commercialization of plant factories, it is necessary to find the optimal set points for the main environmental parameters from the crop development aspects in short and long term bases. Growth and photosynthesis models are powerful tools for supporting decision making for microclimate control to ensure normal growth of plants and consequently high yields with the maximum resource saving in a various production systems (Marcelis, 1998). Modelling of $CO_2$ exchange by plants will provide background to

define and set short term requirements for environment control, whereas modeling of plant growth will provide important information for the prediction of harvest, maximization of production and long term optimal management of plant factory production systems. To our knowledge, researches on photosynthesis and growth modeling for basil and ice plant under closed environment conditions were not accomplished so far.

The objective of this study was to develop photosynthesis and growth models of sweet basil and ice plant in plant factories by using a biochemical model coupled with stomatal conductance and transpiration for photosynthesis and an expo-linear model for growth.

# LITERATURE REVIEW

## *Photosynthesis Model*

The photosynthetic rate of plant was determined by the assimilation of $CO_2$. The modelling of assimilation of $CO_2$ has been gradually developed. For example, de Wit (1965) calculated the total dry matter based on light-photosynthesis [1]

$$A = \alpha \cdot A_{max} \cdot I/(\alpha \cdot I + A_{max}) \quad \text{----------[1]}$$

This model under-estimated the $CO_2$ assimilation rate, so Gourdriaan and van Laar (1978) showed the relation with photosynthetic rate and photosynthetically active radiation (PAR) using negative exponential formulae.

$$A = A_{max} \cdot (1-\exp(-\alpha \cdot I/A_{max})) \quad \text{----------[2]}$$

Thornley (1998) suggested the photosynthetic model based on general non-rectangular hyperbola formulae [3]. This model could describe the ex-

act photosynthetic reaction better than previous models regardless of complexity

$$A = [\alpha \cdot I + A_{max} - ((\alpha \cdot I + A_{max})^2 - 4 \cdot \alpha \cdot I \cdot \theta \cdot A_{max})^{0.5}] / 2\theta \quad \text{---------[3]}$$

Besides photosynthetic models such as negative exponential and non-rectangular hyperbola formulas, a biochemical model (FvCB model) of photosynthetic $CO_2$ assimilation for C3 plant have been developed by Farquhar, von Caemmerer and Berry (Farquhar et al., 1980). FvCB model has been extensively adopted to ecological and physiological studies, for instance, for determination of the effect of elevated $CO_2$ on plant productivity (Medlyn et al, 1999). A coupled model to photosynthesis-stomatal conductance-transpiration has been proposed (Collatz et al., 1995; Nikolov et al., 1995) that unites FvCB model with a model of stomatal conductance (Leuning et al., 1995) and an energy budget balance. This coupled-model considered

both the biochemical limitation for $CO_2$ and the stomatal limitation to supply of $CO_2$.

Sharkey (1985) included the rate of triose phosphate utilization (TPU) as one of important biochemical limitation and Harley (1992) included the TPU limitation in their model. A coupled model of photosynthesis, stomatal conductance and transpiration for roses was realized as a program considering their combined models (Kim et al., 2003).

***Growth Model***

Growth models may be used in decision support systems, greenhouse climate control and prediction and planning of production as discussed by Lentz (1998). In the most growth model, the yield of a crop is determined by dry matter (DM) production, DM distribution and the DM content of the harvestable organs (Marcelis et al, 1998). Most growth models were classi-

fied into descriptive and explanatory models. Descriptive models have a short computing time and they usually contain few state variables such as temperature and accumulated light (Van Strten, 1996). Descriptive growth models are similar to static models such as regression formulas.

Explanatory growth models facilitate comprehension of complex system. Most explanatory biomass models are photosynthesis-based models such as Tomsim and Tomgrow (Heuvelink, 1999). These models are process-oriented, while models based on plant growth analysis are function-oriented models (Gary et al., 1998). Explanatory growth models are similar to dynamic models that predict the change of system and compose of a series of derivative formulas. Dynamic growth models have advantages as an aspect of system prediction comparing with descriptive growth models.

## LITERATURE CITED

De Pury, D.G.G. and G.D. Farquahar. 1997. Simple scaling of photosynthesis from leaves to canopies without the errors of big-leaf models. Plant Cell Environ. 20: 537-557.

Farquhar, G.D. and T.D. Sharkey. 1982. Stomatal conductance and photosynthesis. Ann. Rev. Plant Physiol. 33:317-345.

Gary, C., J.W. Jones, and M. Tchamitchian. 1998. Crop modelling in horticulture: state of the art. Sci. Hort. 74:3-20.

Goto, E. 2012. Plant production in a closed plant factory with artificial lighting. Acta Hort. 956: 37-49.

Harley, P.C., R.B. Thomas, J.F. Reynolds, and B.R. Strain. 1992. Modelling photosynthesis of cotton grown in elevated $CO_2$. Plant Cell Environ. 23: 351-363.

Heuvelink, E. 1999. Evaluation of a dynamic simulation model for tomato crop growth a development. Ann. Bot. 83:413-422.

Kim, P.G., K.Y. Lee, S.D. Hur, S.H. Kim, and E.J. Lee. 2003. Effects of shading treatment on photosynthetic activity of *Acanthopanax senti-*

*cosus*. Kor. J. Ecol. 26: 321-326.

Kim, S.H. and J.H. Lieth. 2003. A coupled model of photosynthesis, stomatal conductance and traspiration for a rose leaf (*Rosa hybrida* L.). Ann. Bot. 91:771-781.

Kozai, T. 2007. Propagation, grafting, and transplant production in closed systems with artificial lighting for commercialization in Japan. J. Ornamental Plants. 7:145-149.

Kozai, T. 2013. Plant factory in Japan – current situation and perspectives. Chronica Horticulturae. 53:8-11.

Lentz, W. 1998. Model applications in horticulture: a review. Sci. Hort. 74:151-174.

Marcelis, L.F.M., E. Heuvelink, and J. Goudriaan. Modelling biomass production and yield of horticultural crops: a review. Sci. Hort. 74:83-111

Sharkey, T.D., C.J. Bernacchi, G. D. Farquhar, and E. L. Sinsaas. 2007. Fitting photosynthetic carbon dioxide response curves for $C_3$ leaves. Plant Cell Environ. 30:1035-1040.

Tesi R., G. Chisci, A. Nencini, and R. Tallarico. 1995. Growth response to fertilization of sweet basil (*Ocimum basilicum* L.). Acta Hort. 390:93-96.

Van Straten, G. 1996. On-line optimal control of greenhouse crop cultivation. Acta Hortic. 406:203-211.

Yeo, K.H. and Y.B. Lee. 2004. The effect of $NO_3^-$-N and $NH_4^+$-N ratio in the nutrient solution on growth and 1uality of sweet basil. Physiol. Plant. 16:889-914.

# CHAPTER I

# Development of a Coupled Photosynthetic Model of Sweet Basil (*Ocimum basilicum* L.) Hydroponically Grown in Plant Factories


## ABSTRACT

For the production of plants in controlled environments such as greenhouses and plant factories, crop modeling and simulations are effective tools for configuring the optimal growth environment. The objective of this study was to develop a coupled photosynthetic model of sweet basil (*Ocimum basilicum* L.) reflecting plant factory conditions. Light response curves were generated using photosynthetic models such as negative exponential, rectangular hyperbola, and non-rectangular hyperbola functions. The light satu-

ration and compensation points determined by regression analysis of light curves using modified non-rectangular hyperbola function in sweet basil leaves were 545.3 and 26.5 μmol·$m^{-2}$·$s^{-1}$, respectively. The non-rectangular hyperbola was the most accurate with complicated parameters, whereas the negative exponential was more accurate than the rectangular hyperbola and could more easily acquire the parameters of the light response curves of sweet basil compared to the non-rectangular hyperbola. The $CO_2$ saturation and compensation points determined by regression analysis of the A-$C_i$ curve were 728.8 and 85.1 μmol·$mol^{-1}$, respectively. A coupled biochemical model of photosynthesis was adopted to simultaneously predict the photo-synthesis, stomatal conductance, transpiration, and temperature of sweet basil leaves. The photosynthetic parameters, maximum carboxylation rate,

potential rate of electron transport, and rate of triose phosphate utilization determined by Sharkey's regression method were 102.6, 117.7, and 7.4 $\mu mol \cdot m^{-2} \cdot s^{-1}$, respectively. Although the A-$C_i$ regression curve of the negative exponential had higher accuracy than the biochemical model, the coupled biochemical model enable to physiologically explain the photosynthesis of sweet basil leaves.

*Additional Keywords*: negative exponential, non-rectangular hyperbola, *Ocimum basilicum* L., transpiration

# INTRODUCTION

The cultivation and consumption of high-quality herbal crops are increasing with improvements in income (Yeo and Lee, 2004). Sweet basil (*Ocimum basilicum* L.) has year-round popularity among consumers (Tesi et al., 1995). Plant factories with artificial lights, in which environmental factors such as light, temperature, humidity, and $CO_2$ can be controlled, enable stable year-round production, regardless of climate conditions (Son, 1993). Crop modeling and simulation are effective tools for planning plant production due to their usefulness in optimizing the environments in greenhouses and plant factories (Heuvelink, 1999).

Photosynthetic models are fundamental modules in crop growth modeling to include environmental factors such as light, $CO_2$ concentration, and

temperature. Such models are classified into descriptive and biochemical types. The descriptive type of model has the advantage of summarizing the photosynthetic characteristics of crops, while the biochemical type is based on the reaction rate of photosynthetic enzymes and critical limiting rates. A biochemical model called the Farquhar, von Caemmerer and Berry (FvCB) model for C3 plants was developed by Farquhar et al. (1980) and has since been widely applied to ecological and physiological research (Medlyn et al, 1999). This model has been improved by inclusion of the rate of triose phosphate utilization (TPU) as an important biochemical limitation (Harley et al., 1992; Sharkey et al., 2007). However, this model is unable to reflect actual crop growth conditions in greenhouses, in which stomatal opening is affected by various environmental factors.

A coupled model of photosynthesis has been developed by combining the FvCB model with stomatal conductance (Leuning, 1995; Nikolov et al., 1995) and energy budget balance (Kim and Lieth, 2003) models. The coupled photosynthetic model considers the biochemical limitations of $CO_2$ carboxylation as well as the stomatal limitations to the $CO_2$ supply. Kim and Lieth (2003) developed a coupled model of photosynthesis, stomatal conductance, and transpiration for roses.

Although simple biochemical model for purple basil photosynthesis has been reported by Polyakova (2015), a coupled biochemical model describing actual photosynthetic activity has not been developed. The objective of this study was to develop descriptive and a coupled model of photosynthesis,

stomatal conductance, and the transpiration of sweet basil combined with sub-models of stomatal conductance and energy balance.

## MATERIALS AND METHODS

### *Plant Materials and Cultivation Conditions*

Sweet basil (*Ocimum basilicum* L.) seeds were sown on a rock-wool tray (600 mm × 400 mm) on May 12$^{th}$, 2014 in venlo-type greenhouses at the Protected Horticulture Research Institute, Rural Development Administration (RDA) located in Busan, Korea. The seedlings of sweet basil with three to four leaves were transplanted on polystyrene panels (100 mm × 100 mm, φ3 cm) on June 2$^{nd}$, 2014. The nutrient solution composition for sweet basil was: $NO_3^-$-N 11.6, $NH_4^+$-N 1.2, P 3.6, K 5.8, Ca 5.8, and Mg 3.0 in meq·L$^{-1}$, and had an EC of 1.5 dS·m$^{-1}$ (Yeo and Lee, 2004). The hydroponic systems (460 mm × 300 mm × 210 mm) used a deep flow technique at a depth of 70 mm. The nutrient solutions were continuously supplied to the cultivation

beds every 10 min at one-hour intervals to maintain the water level in the hydroponic systems. The experiment was conducted in a container-type plant factory (3 m × 12 m). Set-points of room temperature, relative humidity, and $CO_2$ concentration inside the container-type plant factory were 20°C, 65%, and 400 $\mu mol \cdot mol^{-1}$, respectively. The light/dark period was 18 h/6 h and photosynthetic photon flux density (PPFD) was maintained at 150 $\mu mol \cdot m^{-2} \cdot s^{-1}$ during the light period. Thirty W bar-type LEDs (PGL-PFL600, Parus, Cheonan, Korea) with a 3:7 mixture of blue (445 nm peak) and red (660 nm peak) were used as artificial light sources. The spectral distribution of the light source is shown in Fig. I-1.

***Photosynthetic and Optical Properties of Sweet Basil Leaves.***

The reflectance and transmittance of sweet basil leaves in 300 - 1,100 nm wavebands at 1 nm intervals were measured on June 29$^{th}$ using a portable spectro-radiometer with an external integrating sphere (LI-1800, Li-Cor, Lincoln, NE, USA). The reflectance was derived by comparing the wall illumination of the sphere caused by a focused beam of radiation reflected from the leaves. The transmittance was derived by comparing the wall illumination caused by the same radiation that was transmitted through the leaves. The absorbance was calculated as 1 – transmittance – reflectance. The measurements were performed only for the top sides of the leaves.

The net $CO_2$ assimilation rate and stomatal conductance to water vapor were measured using a portable photosynthesis system (LI-6400, Li-Cor, Lincoln, NE, USA) equipped with an infrared gas analyzer. Fully developed basil leaf was placed across the 6 $cm^2$ leaf chamber. The temperature of the leaf chamber was maintained at 25 ºC and relative humidity at 60-70% dur-

ing the measurements. The net $CO_2$ assimilation rate as a function of light curves was determined at each step every three to four minutes. Variable PPFDs were beamed from an internal LED light source giving a PPFD range from 0 to 1500 µmol · $m^{-2}$ · $s^{-1}$ at 400 µmol · $mol^{-1}$ of $CO_2$ concentration. Regression analyses for descriptive models were conducted for negative exponential (Evans et al., 1993; Eq. I-1), rectangular hyperbola (de Wit, 1965; Eq. I-2), non-rectangular hyperbola (Thornley, 1976; Eq. I-3), and modified non-rectangular (Eq. I-4) models, as described below:

$$A=A_{max} \cdot \{(1-\exp(-\alpha \cdot I / A_{max}))\} - R_d \qquad \text{(Eq. I-1)}$$

$$A = \alpha \cdot A_{max} \cdot I / (\alpha \cdot I + A_{max}) - R_d \qquad \text{(Eq. I-2)}$$

$$A=[\alpha \cdot I+A_{max} - \{(\alpha \cdot I+A_{max})^2 - 4\alpha \cdot I \cdot \theta \cdot A_{max}\}^{05}]/2\theta - R_d \qquad \text{(Eq. I-3)}$$

$$A = [\alpha \cdot I + A_{max} - \{(\alpha \cdot I + A_{max})^2 - 4\alpha \cdot I \cdot A_{max}\}^{0.5}] / 2\theta - R_d \qquad \text{(Eq. I-4)}$$

where A is the net $CO_2$ assimilation rate ($\mu mol \cdot m^{-2} \cdot s^{-1}$), $A_{max}$ is the maximum net $CO_2$ assimilation rate ($\mu mol \cdot m^{-2} \cdot s^{-1}$), $\alpha$ parameter is the initial slope, I is the photosynthetic photon flux ($\mu mol \cdot m^{-2} \cdot s^{-1}$), Rd is the respiration rate ($\mu mol \cdot m^{-2} \cdot s^{-1}$), and $\theta$ is the curvature of the photosynthetic curve.

The net $CO_2$ assimilation rate as a function of the A-$C_i$ curve was determined at each step every three to four minutes. Variable $CO_2$ concentrations were maintained from the photosynthesis measurement system, which resulted in $CO_2$ concentrations ranging from 100 to 1,500 $\mu mol \cdot mol^{-1}$ at 500 $\mu mol \cdot m^{-2} \cdot s^{-1}$ of PPFD. Sharkey's method (2007) was used to solve the parameters of biochemical models.

***A Coupled Biochemical Model of Sweet basil Photosynthesis***

Biochemical models (Eq. I-5 to I-8) were used to acquire the net photosynthetic rate, which has limitations such as the rates of $CO_2$ carboxylation by Rubisco, Ribulose 1,5-bisphophate (RuBP) regeneration, and triose phosphate utilization.

$$A = \min\{A_c,\ A_j,\ A_p\} - R_d \qquad \text{(Eq. I-5)}$$

$$A_c = V_{max} \frac{C_i - \tau^*}{C_i + K_c \cdot (1 + \frac{O}{K_O})} \qquad \text{(Eq. I-6)}$$

$$A_j = \frac{J \cdot (C_i - \tau^*)}{4\ (C_i + 2\ \tau^*)} \qquad \text{(Eq. I-7)}$$

$$A_p = 3 \cdot TPU \qquad \text{(Eq. I-8)}$$

where $A_c$ is rubisco-limited photosynthetic rate, $A_j$ is RuBP regeneration limited photosynthetic rate through electron transport, $A_p$ is TPU limited photosynthetic rate, $V_{max}$ is the maximum rate of Rubisco carboxylation ($\mu mol \cdot m^{-2} \cdot s^{-1}$), $C_i$ is the intercellular $CO_2$ concentration ($\mu mol \cdot mol^{-1}$), $\tau^*$ is the $CO_2$ compensation point in the absence of $R_d$ ($\mu mol \cdot mol^{-1}$), $K_c$ and $K_o$ are the Michaelis-Menten constants of Rubisco for $CO_2$ and $O_2$, respectively ($\mu mol \cdot mol^{-1}$), O is the oxygen partial pressure ($\mu mol \cdot mol^{-1}$), J is the electron transport rate ($\mu mol \cdot m^{-2} \cdot s^{-1}$), and TPU is the triose phosphate utilization rate ($\mu mol \cdot m^{-2} \cdot s^{-1}$).

The intercellular $CO_2$ concentration in sweet basil leaves was measured by the portable photosynthetic measurement system. Eq. I-9 describes the estimating equation (Caemmerer and Farquhar, 1981).

$$c_i = \frac{\left(g_{tc} - \frac{E}{2}\right) \cdot C_a - A}{g_{tc} + E/2} \qquad \text{(Eq. I-9)}$$

where $g_{tc}$ is total conductance to $CO_2$ (μmol· $mol^{-1}$) and E is transpiration (mol· $m^{-2}$· $s^{-1}$).

The stomatal conductance was obtained by the Ball, Woodrow and Berry (BWB) model (Ball et al., 1987) and the relative humidity at leaf surface ($h_s$) was described as a linear function (Eq. I-10). The photosynthetic limitation of sweet basil leaves was calculated using an Excel macro program developed by Sharkey et al. (2007).

$$g_s = b + m \cdot A \frac{h_s}{\left(\frac{C_s}{C_a}\right)} \qquad \text{(Eq. I-10)}$$

where $g_s$ ($mol \cdot m^{-2} \cdot s^{-1}$) is the stomatal conductance to water vapor, b ($mol \cdot m^{-2} \cdot s^{-1}$) is the minimum stomatal conductance to water vapor at the light compensation point in the BWB model, m is the empirical coefficient for the sensitivity of $g_s$, $C_s$ and $C_a$ the ambient air and leaf surface $CO_2$ concentrations ($\mu mol \cdot mol^{-1}$), respectively. Parameter $h_s$ is the relative humidity at leaf surface, and A is net assimilation rate of $CO_2$.

The energy balance model was used to estimate the leaf temperature as a function of $g_s$, boundary layer conductance, and the environmental parameters such as air temperature, relative humidity, and radiation. The three submodels of FvCB, BWB, and energy balance were interdependent. The FvCB model used $C_i$ and the leaf temperature ($T_L$) and included the photosynthetic active radiation value. The BWB model required the net photosynthetic rate (A) and $C_i$. $T_L$ was estimated iteratively from the energy balance using the air temperature ($T_a$), conductance for heat, and water vapor. Initially, $T_L$ and

$C_i$ were assumed to be equal to $T_a$ and $0.7C_a$, respectively, in order to obtain and estimate A, which was then used to obtain $g_s$. $C_i$ was estimated using the resulting A and $g_s$. These processes were solved iteratively using the Newton-Raphson method until $C_i$ and $T_L$ became stable (Kim and Lieth, 2003).

## RESULTS AND DISCUSSION

Light response curves of sweet basil leaves generated by varying light intensities are shown in Fig. I-2. The range at which photosynthetic increases no longer occur due to light increases is the light saturation point. The net $CO_2$ assimilation rates in the leaves of sweet basil were saturated at about 500 $\mu mol \cdot m^{-2} \cdot s^{-1}$ PPFD, following the initial linear increases with an increasing PPFD around 200 $\mu mol \cdot m^{-2} \cdot s^{-1}$ (Fig. I-2). The relationship between

light intensity and the photosynthetic rate with 100 μmol·m$^{-2}$·s$^{-1}$ PPFD was linear, as reported by Sharp et al. (1984).

Parameters of the negative exponential and rectangular hyperbola models were estimated using regression analysis (Table I-1). The negative exponential model ($R^2$=0.999) was more accurate for describing the light curve than the rectangular hyperbola model ($R^2$=0.993). In addition, the rectangular hyperbola overestimated the photosynthetic value around the light saturation point more than the negative exponential model (de Wit, 1965; Goudriaan and van Laar, 1978). The initial slope ($\alpha$) of the non-rectangular hyperbola (Eq. I-3) was 52.0±1.92, determined from the measured photosynthetic values ranging from 0 to 100 μmol·m$^{-2}$·s$^{-1}$ PPFD. The parameters of the negative exponential model were applied to the non-rectangular hyperbola model for curvatures from 200 to 1,500 μmol·m$^{-2}$·s$^{-1}$ PPFD. The average curvature

($\theta$) of the non-rectangular hyperbola (Eq. I-3) for the light curve was 0.80±0.03 by non-linear regression analysis. Thus the low accuracy in the rectangular hyperbola could be compensated for by the non-rectangular hyperbola. Modified non-rectangular hyperbola model has proper method for describing light saturation point using regression analysis without asymptote (Fig. I-3, Table I-2)

The residual sum of squares between measured and predicted photosynthetic rates was the lowest at the non-rectangular hyperbola among the three models. The non-rectangular hyperbola showed more accurate predictions under 1,000 $\mu mol \cdot m^{-2} \cdot s^{-1}$ PPFD and under-estimated predictions over 1,000 $\mu mol \cdot m^{-2} \cdot s^{-1}$ PPFD compared to the negative exponential model (Fig. I-2). The non-rectangular hyperbola and the negative exponential models had

higher levels of accuracy than the rectangular hyperbola, and the negative exponential model was enough for describing the light curve.

Regression analysis was applied to the measured photosynthetic rates with increases in $CO_2$ concentration using the negative exponential model (Fig. I-4). The y-axis and x-axis values of the intercept as the estimates of $R_p$ and $C_{comp}$ were 7.9 $\mu mol \cdot m^{-2} \cdot s^{-1}$ and 85.1 $\mu mol \cdot m^{-2} \cdot s^{-1}$. When the intercellular $CO_2$ concentrations were 62.1 $\mu mol \cdot mol^{-1}$ at the compensation point and 518.8 $\mu mol \cdot mol^{-1}$ at the saturation point, their $CO_2$ concentrations ($C_{comp}$ and $C_{sat}$) of atmosphere were 85.1 and 728.8 $\mu mol \cdot mol^{-1}$, respectively (Table I-3). The photosynthetic limitation curve (Fig. I-5) of sweet basil leaves was obtained using Sharkey's method (2007). As shown in Fig. I-5 the predicted intercellular $CO_2$ concentrations ranged from 100 to 200 $\mu mol \cdot mol^{-1}$ when determined based on the photosynthetic rate predicted us-

ing Rubisco carboxylation rate, from 200 to 400 μmol·mol$^{-1}$ when determined using the Ribulose 1,5-bisphosphate (RuBP) regeneration rate, and from 400 to 1,000 μmol·mol$^{-1}$ when determined using the triose phosphate utilization rate. It was concluded that the sweet basil photosynthetic A-$C_i$ curve is appropriate to fit the parameters used in Sharkey's method.

The maximum carboxylation rate ($V_{max}$, μmol·m$^{-2}$·s$^{-1}$), the maximum rate of electron transport ($J_{max}$, μmol·m$^{-2}$·s$^{-1}$), the triose phosphate utilization rate (TPU, μmol·m$^{-2}$·s$^{-1}$), and the mitochondrial respiration in the light ($R_d$, μmol·m$^{-2}$·s$^{-1}$) were 102.6, 117.7, 7.4, and 0.7, respectively (Table I-4). These parameters of sweet basil were similar to those of roses calculated by Kim and Lieth (2003), but considerably different from those of purple basil (cv 'Ararat') determined by Polyakakova et al. (2015). These differences

might be related differences in cultivars and environmental conditions, such as light sources.

The parameters of minimum stomatal conductance to water vapor at the light compensation point (b) and the empirical coefficient for the sensitivity of $g_s$, to A, $C_s$ and $h_s$ in the BWB model (m) were solved with linear regression analysis using the measured A-$C_i$ values of sweet basil leaves (Table I-4). The parameters of the m value showing the stomatal conductance slope were considerably lower than those of a rose, emphasizing those A-Ci curves should be acquired according to various conditions. The photosynthetic rates could be acquired by inputting their parameters and optical characteristics of sweet basil into the photosynthetic simulator developed by Kim and Lieth (2003).

Overall the residual sum of squares between measured and predicted photosynthetic rates from the coupled biochemical model of photosynthesis, stomata conductance, and transpiration was larger than the residual sum of squares using the negative exponential model (Table I-5). The biochemical model underestimated the photosynthetic rate compared to the negative exponential model at a high concentration of $CO_2$. However, the coupled biochemical model was very effective for physiologically explain sweet basil photosynthesis considering environmental factors and stomatal conductance.

Table I-1. Photosynthetic parameters of the rectangular hyperbola (Eq. I-1) and negative exponential (Eq. I-2) models calculated from the light response curves of sweet basil in Fig. I-2.

| Parameter | Negative exponential model ($R^2$=0.999) | Rectangular hyperbola model ($R^2$=0.993) |
|---|---|---|
| $A_{max}$ ($\mu mol \cdot m^{-2} \cdot s^{-1}$)[z] | 23.9±2.04 | 31.0±2.92[u] |
| $\alpha$ ($mmol \cdot mol^{-1}$)[y] | 62.1±1.25 | 79.9±0.86 |
| $R_d$ ($\mu mol \cdot m^{-2} \cdot s^{-1}$)[x] | 2.1±0.07 | 2.4±0.09 |
| $L_{comp}$ ($\mu mol \cdot m^{-2} \cdot s^{-1}$)[w] | 34.7±0.33 | 33.0±0.64 |
| $L_{sat}$ ($\mu mol \cdot m^{-2} \cdot s^{-1}$)[v] | 479.0±25.66 | 493.4±38.71 |

[z]Maximum photosynthetic capacity; [y]Apparent quantum yield.

[x]Dark respiration rate.

[w]Light compensation point.

[v]Light saturation point.

[u]Mean ± standard error (n=3).

Table I-2. Photosynthetic parameters of non-rectangular hyperbola (Eq. I-3) and modified non-rectangular hyperbola (Eq I-4) models calculated from the light response curves of sweet basil in Fig. I-3.

| Parameter | Non-rectangular hyperbola (R2=0.999) | Modified non-rectangular hyperbola ($R^2$=0.993) |
|---|---|---|
| $A_{max}$ ($\mu mol \cdot m^{-2} \cdot s^{-1}$)[z] | 24.9±2.07t | 28.1±2.56 |
| $\alpha$ ($mmol \cdot mol^{-1}$)[y] | 52.0±1.92 | 52.0±1.92 |
| $\theta$ [x] | 0.8±0.03 | 1.4±0.03 |
| $R_d$ ($\mu mol \cdot m^{-2} \cdot s^{-1}$) [w] | 1.8±0.09 | 1.0±0.18 |
| $L_{comp}$ ($\mu mol \cdot m^{-2} \cdot s^{-1}$) [v] | 28.6±2.14 | 26.5±5.11 |
| $L_{sat}$ ($\mu mol \cdot m^{-2} \cdot s^{-1}$)[u] | 419.8±18.69 | 545.3±48.15 |

[z]Maximum photosynthetic capacity; [y]Apparent quantum yield; [x]Curvature of curve; [w]Dark respiration rate.

[v]Light compensation point.

[u]Light saturation point.

[t]Mean ± standard error (n=3).

Table I-3. Photosynthetic parameters of the negative exponential model (Eq. I-2) calculated from the A-$C_i$ curves of sweet basil in Fig. I-4.

| Parameter | Negative exponential model ($R^2$=0.992) |
|---|---|
| $A_{max}$ ($\mu mol \cdot m^{-2} \cdot s^{-1}$)[z] | 30.3±0.18[u] |
| $\alpha$ ($mmol \cdot mol^{-1}$)[y] | 148.2±20.76 |
| $R_d$ ($\mu mol \cdot m^{-2} \cdot s^{-1}$)[x] | 7.9±0.95 |
| $C_{comp}$ ($\mu mol \cdot mol^{-1}$)[w] | 85.1±0.37 |
| $C_{sat}$ ($\mu mol \cdot mol^{-1}$)[v] | 728.8±34.58 |

[z]Maximum photosynthetic capacity; [y]Apparent quantum yield; [x]Mitochondrial respiration in the light.

[w]$CO_2$ compensation point.

[v]$CO_2$ saturation point.

[u]Mean ± standard error (n=3).

Table I-4. Estimated photosynthetic parameters of the biochemical model of sweet basil at a leaf temperature of 26.9°C.

| Parameter | $V_{max}$[z] ($\mu mol \cdot m^{-2} \cdot s^{-1}$) | $J_{max}$[y] ($\mu mol \cdot m^{-2} \cdot s^{-1}$) | TPU[x] ($\mu mol \cdot m^{-2} \cdot s^{-1}$) | $R_d$[w] ($\mu mol \cdot m^{-2} \cdot s^{-1}$) | b[v] ($mol \cdot m^{-1} \cdot s^{-1}$) | m[u] |
|---|---|---|---|---|---|---|
| Value | 102.6±1.54[t] | 117.9±1.16 | 7.4±0.14 | 0.7±0.16 | 0.3172 | 0.00006 |

[z]Maximum carboxylation rate.

[y]Maximum rate of electron transport.

[x]Triose phosphate utilization rate.

[w]Mitochondrial respiration in the light.

[v]Minimum stomatal conductance to water vapor at the light.

[u]Empirical coefficient for the sensitivity of $g_s$ to A, $C_s$ and $h_s$ in the BWB model

[t]Mean ± standard error (n=3)

Table I-5. Comparison of the residual sum of squares between negative exponential and biochemical models and sweet basil.

| $C_i^z$ ($\mu mol \cdot mol^{-1}$) | Measured value ($\mu mol \cdot m^{-2} \cdot s^{-1}$) | Predicted value ($\mu mol \cdot m^{-2} \cdot s^{-1}$) | |
|---|---|---|---|
| | | Negative exponential model | Biochemical model |
| 77 | 2.1 | 1.6 | 3.7 |
| 135 | 6.1 | 6.7 | 9.2 |
| 203 | 10.1 | 11.1 | 12.2 |
| 260 | 13.5 | 13.9 | 14.0 |
| 484 | 14.5 | 19.5 | 16.5 |
| 844 | 21.3 | 21.8 | 17.8 |
| Residual sum of squares | - | 26.7 | 33.4 |

[z]Intercellular $CO_2$ concentration.

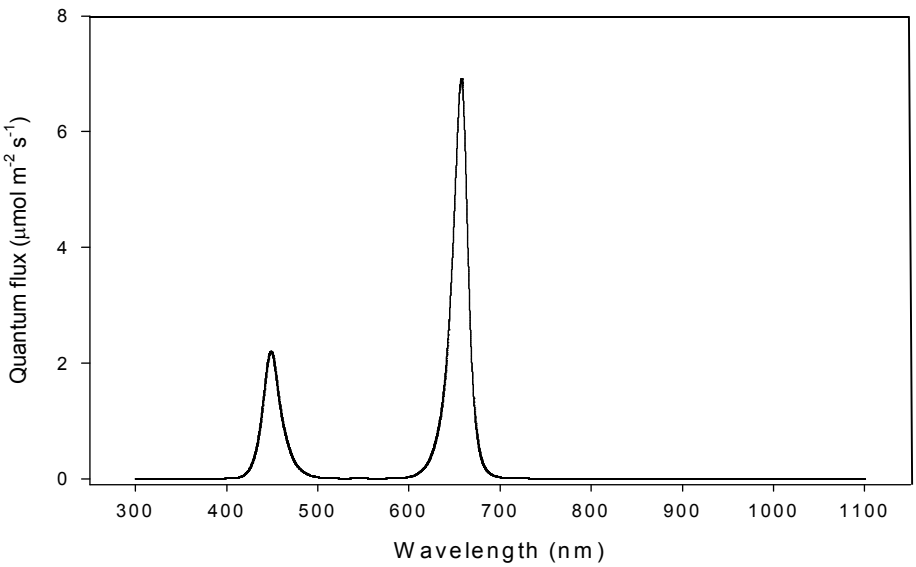


Fig. I-1. Spectral distribution of mixed (blue : red = 3:7) light-emitting diode (LED) lights at a distance of 20cm from the light source in a closed-type plant factory.

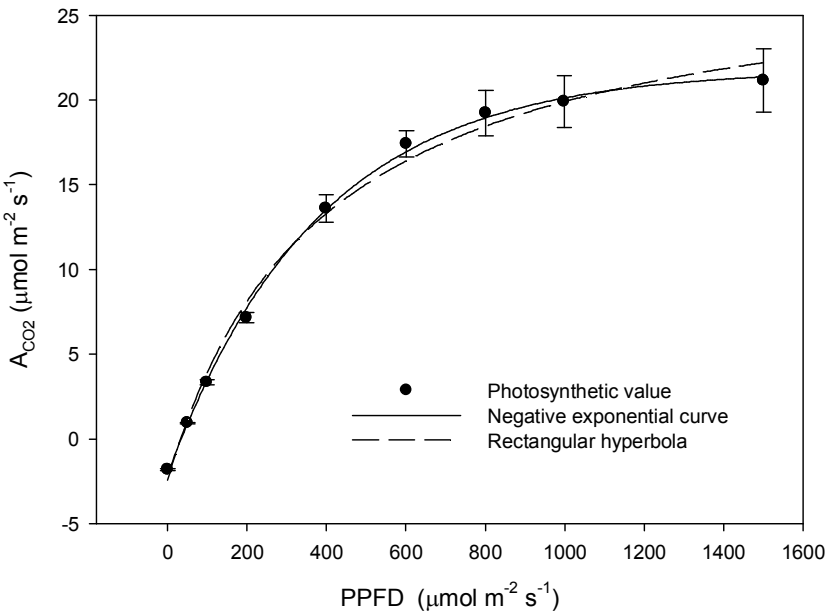


Fig. I-2. Regression curves of light response using negative exponential and rectangular hyperbola models at a $CO_2$ concentration of 400 μmol·$mol^{-1}$ in the leaves of sweet basil. Vertical bars are standard errors of the means from three replications. $A_{CO2}$ and PPFD are the $CO_2$ assimilation rate and the photosynthetic photon flux, respectively.

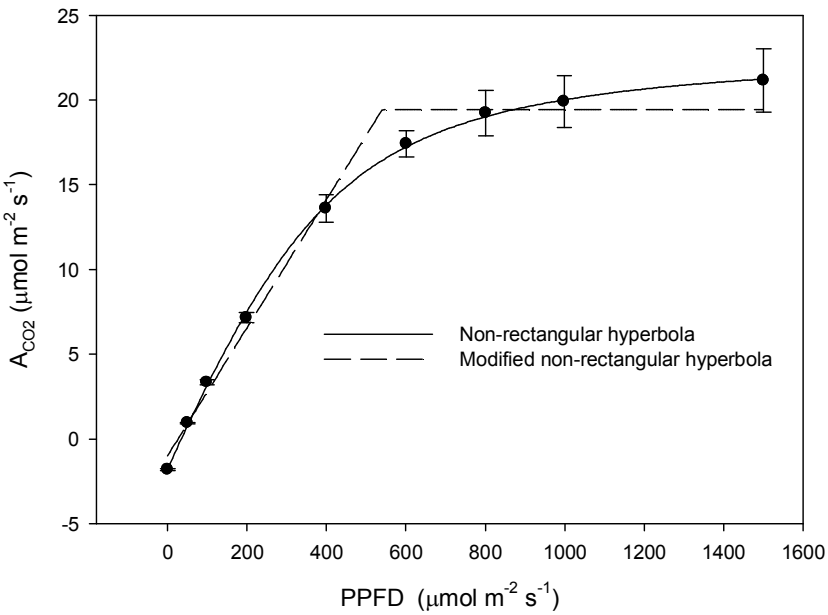


Fig. I-3. Regression curves of light response using rectangular hyperbola and non-rectangular hyperbola models at a $CO_2$ concentration of 400 μmol·$mol^{-1}$ in the leaves of sweet basil. Vertical bars are standard errors of the means from three replications. $A_{CO2}$ and PPFD are the $CO_2$ assimilation rate and the photosynthetic photon flux, respectively.

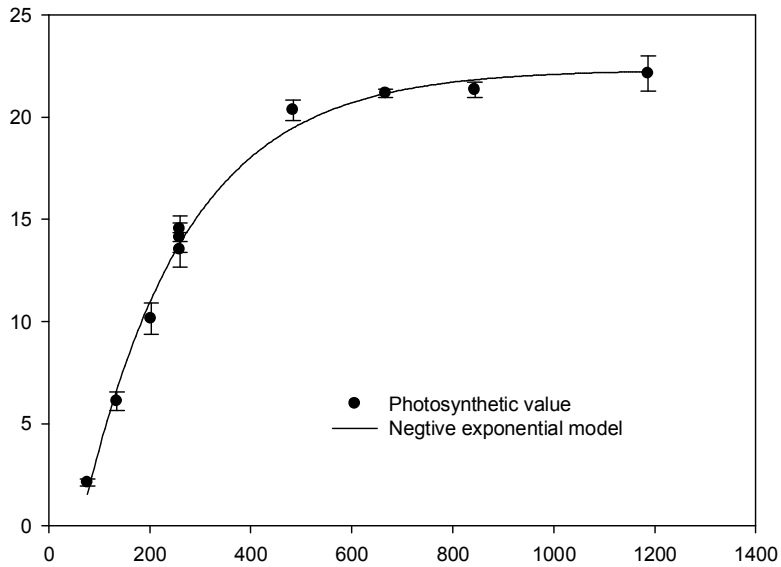


Fig. I-4. Net $CO_2$ assimilation rate (A) as a function of the intercellular $CO_2$ concentration in the leaves of sweet basil at a photosynthetic photon flux density of 500 $\mu mol \cdot m^{-2} \cdot s^{-1}$. Vertical bars are the standard errors of the means from the three replications.

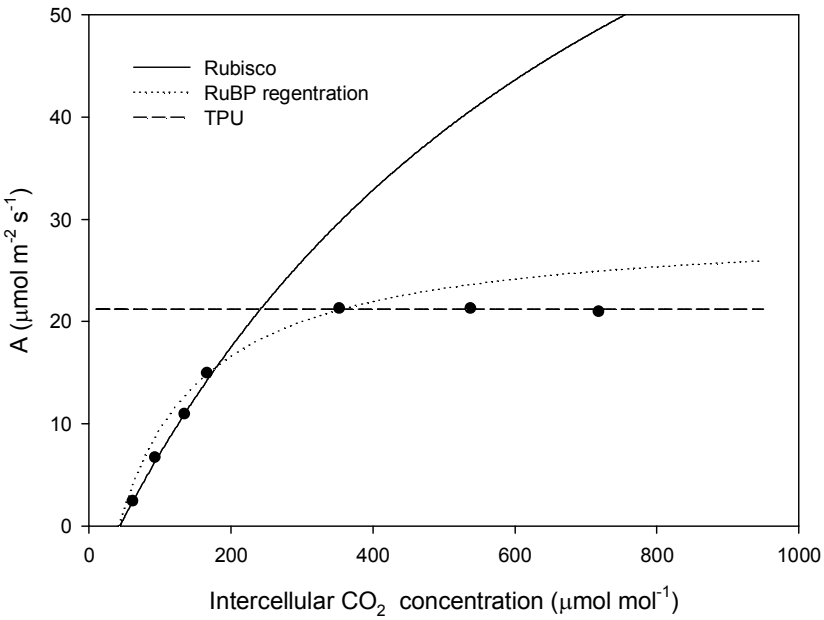


Fig. I-5. Predicted net $CO_2$ assimilation rate (A) as a function of intercellular $CO_2$ concentration in the leaves of sweet basil at a photosynthetic photon flux density of 500 $\mu mol \cdot m^{-2} \cdot s^{-1}$. Prediction of photosynthesis assumed Rubisco, RuBP, or TPU limitation.

## LITERATURE CITED

Ball, J.T., I.E. Woodrow, and J.A. Berry. 1987. A model predicting stomatal conductance and its contribution to the control of photosynthesis under different environmental conditions. Progress in photosynthesis research p.221-224. In : Biggins J(ed). Prog. Photosyn. Res. Martinus Nijihoff Publishers, The Netherlands.

de Wit, C.T. 1965. Photosynthesis of leaf canopies. Agricultural Reports 663. Pudoc, Wageningen.

Evans, J.R., I. Jakobsen, and E. Orgren. 1993. Photosynthetic light-response curves 2: Gradients of light absorption and photosynthetic capacity. Planta 189:191-200.

Farquhar, G. D., S. von Caemmerer and J. A. Berry. 1980. A biochemical model of photosynthetic $CO_2$ assimilation in leaves of C3 species. Planta 149: 78-90

Goudriaan, J. and H.H. van Laar. 1978. Calculation of daily totals of the gross $CO_2$ assimilation of leaf canopies. NL. J. Agr. Sci. 26:373-382.

Harley, P.C., R.B. Thomas, J.F. Reynolds, and B.R. Strain. 1992. Modelling photosynthesis of cotton grown in elevated $CO_2$. Plant Cell Environ. 23:

351-363.

Heuvelink, E. 1999. Evaluation of a dynamic simulation model for tomato crop growth a development. Ann. Bot. 83: 413-422.

Kim, P.G., K.Y. Lee, S.D. Hur, S.H. Kim, and E.J. Lee, 2003. Effects of shading treatment on photosynthetic activity of *Acanthopanax senticosus*. Kor. J. Ecol. 26: 321-326.

Kim, S.H. and J.H. Lieth. 2003. A coupled model of photosynthesis, stomatal conductance and traspiration for a rose leaf (*Rosa hybrida* L.). Ann. Bot. 91: 771-781.

Leuning, R. 1995. A critical appraisal of a combined stomatal-photosynthesis model. Plant Cell Environ. 18:339-355.

Medlyn, B.E., F.W. Badeck, D.G.G. de Pury, C.V.M. Barton, and M. Broadmeadow. 1999. Effects of elevated $CO_2$ on photosynthesis in European forest species: a meta-analysis of model parameters. Plant Cell Environ. 22: 1475-1495.

Nikolov, N.T., W.J. Massman, and A.W. Shoettle. 1995. Coupling biochemical and biophysical processes at the leaf level: an equilibrium photosynthesis model for leaves of C3 plants. Ecol. Modell 80: 205-235.

Polyakova, M.N., Y.T. Martirosyan, T.A. Dilovaova, and A.A. Kosobryu-

khov. 2015. Photosynthesis and productivity of basil plants (*Ocimum basilicum* L.) under different irradiation. Agri. Biol. 50:124-130.

Sharkey, T.D., C.J. Bernacchi, G.D. Farquhar, and E.L. Sinsaas. 2007. Fitting photosynthetic carbon dioxide response curves for C3 leaves. Plant Cell Environ. 30:1035-1040.

Sharp, R.E., M.A. Mattews, and J.J. Boyer. 1984. Kok effect and the quantum yield of photosynthesis. Plant Physiology 75:95-101.

Son, J.E. 1993. Plant factory - A prospective urban agriculture. J. Bio. Fac. Environ. 2:69-76.

Thornley, J. H. M. 1976. Mathematical models. Plant physiology, Academic press. London. P. 318.

Tesi, R., G. Chisci, A. Nencini, and R. Tallarico. 1995. Growth response to fertilization of sweet basil (*Ocimum basilicum* L.). Acta Hortic. 390:93-96.

Yeo, K.H. and Y.B. Lee. 2004. The Effect of $NO_3^-$-N and $NH_4^+$-N ratio in the nutrient solution on growth and quality of sweet basil. Kor. J. Hortic. Sci. Technol. 22:37-42.

# CHAPTER II

# DEVELOPMENT OF A COUPLED MODEL OF PHOTOSYNTHESIS AND STOMATAL CONDUCTANCE FOR ICE PLANT, A FACULTATIVE CAM PLANT IN PLANT FACTORIES

## ABSTRACT

The ice plant (*Mesembryanthemum crystallinum* L.), a medicinal plant with well-known retarding effects on diabetes mellitus, is increasingly being produced in plant factories in Asia. Ice plant is a CAM (Crassulacean Acid Metabolism) plant, but known as performing $C_3$ photosynthesis during the juvenile period. The objective of this study was to develop a photosynthetic model of ice plant under plant factory conditions. A $C_3$ photosynthesis was performed under growth conditions of plant factory corresponding to juve-

nile stage, while conversion from $C_3$ to CAM was observed under a stressed condition of EC 6.0dS·m$^{-1}$. The light saturation and compensation points, determined by the regression analysis of $C_3$ light curves for the ice plant leaves, were 609.37 and 53.17 μmol·m$^{-2}$·s$^{-1}$, respectively. The accuracy of the light response was compared between negative exponential and non-rectangular hyperbola functions. The non-rectangular hyperbola was more accurate with complicated parameters, while the negative exponential function could more easily acquire the parameters of the light response curves for ice plant. The $CO_2$ saturation and compensation points, determined by the regression analysis of the A-Ci curve, were 632.91 and 117.19 μmol·mol$^{-1}$, respectively. A coupled photosynthetic model was developed for simultaneous prediction of the photosynthesis, stomatal conductance, transpiration, and temperature of ice plant leaves. Sharkey's regression

method was used to determine the photosynthetic parameters of maximum carboxylation rate, potential rate of electron transport, and rate of triose phosphate utilization, which were 222.3, 234.9, and 13.0, $\mu mol \cdot mol^{-1}$, respectively. The parameters of minimum stomatal conductance of water vapor at the light compensation point (b) and the empirical coefficient (m) for the sensitivity of $g_s$, to A, $C_s$ and $h_s$ in the Ball, Woodrow and Berry(BWB) model could be solved as b=0.0487 and m=0.0012 by linear regression analysis using the measured A-Ci values. The coupled biochemical model was more effective for explaining the $C_3$ photosynthesis of ice plant in the juvenile stage under plant factory conditions.

*Additional Key words*: biochemical model, light compensation point, light saturation point, *Mesembryanthemum crystallinum* L., negative exponential curve, non-rectangular hyperbola.

# INTRODUCTION

The ice plant (*Mesembryanthemum crystallinum* L.), a member of the *Aizoaceae* family, synthesizes a polyol in the leaf that imparts antioxidant properties, making this plant increasingly attractive for plant factory production in Asia. In addition, the ice plant contains abundant inositol, $\beta$-glucan, and various minerals, but inositol is of particular interest because it can aid in the treatment of diabetes mellitus (Cha et al., 2014). The commercialization of inositol production from raw materials in plant factories is therefore being actively pursued.

The ice plant is particularly well known for performing Crassulacean Acid Metabolism (CAM), common in succulent plants such as cactus. Winter et al. (1978) reported a seasonal shift from $C_3$ photosynthesis to CAM plant. Cushman (2001) later reported that the ice plant performs $C_3$ photosynthesis during its juvenile stage. Ice plants grown in plant factory condi-

tions are harvested at this juvenile stage because the leaves are shrunken during the adult stage. Therefore, crop modeling and simulation of these plants in their juvenile stage are needed, in order to optimize the environments of greenhouses and plant factories for planned production (Heuvelink, 1999).

Photosynthetic models are fundamental parts of crop growth models and are classified into descriptive and biochemical types. The descriptive model summarizes the photosynthetic characteristics of the crop, while the biochemical model is based on the reaction rate of the photosynthetic enzymes and critical limiting rates. The Farquhar, von Caemmerer and Berry(FvCB, 1980) model for C3 plants, as a biochemical model, has been widely applied to physiological research (Medlyn et al, 1999). This model has been made more informative by incorporating the rate of triose phosphate utilization (TPU) and the TPU limitation (Harley et al., 1992; Sharkey et al., 2007).

However, this kind of model does not reflect the actual crop growth conditions in greenhouses; for instance, the actual state of stomatal opening affecting photosynthetic efficiency under changing environment conditions. A coupled model of photosynthesis has therefore been developed that combines the FvCB model with stomatal conductance (Leuning, 1995; Nikolov et al., 1995) and energy budget balance (Kim and Lieth, 2003) models. Ball (1987) suggested that photosynthetic rate has a strong linear relationship with stomatal conductance. The coupled photosynthetic model therefore considers the biochemical limitations of $CO_2$ carboxylation as well as the stomatal limitations to the $CO_2$ supply. Kim and Lieth (2003) developed a coupled model of photosynthesis, stomatal conductance, and transpiration for roses.

Photosynthesis modeling using biochemical models has not yet been conducted for the ice plant as a CAM plant, although the malate content at

each growth stage has been analyzed for determining CAM activation and has confirmed that its photosynthesis is exclusively $C_3$ during the juvenile stage (Winter et al., 1978). The objective of the present study was to develop descriptive and coupled models of photosynthesis and stomatal conductance of the ice plant that combined sub-models of stomatal conductance and energy balance.

## MATERIALS AND METHODS

### *Plant Materials and Cultivation Conditions*

Seeds of ice plant were sown on a rock-wool tray (600 mm ×400 mm) on May 12$^{th}$, 2014 in velno-type greenhouses of the Protected Horticulture Research Station, Rural Development Administration (RDA) located in Busan, Korea. Ice plant seedlings at the 3-4 leaf stage were transplanted on polystyrene panels (100 × 100 mm, Φ 3cm) on June 2$^{nd}$, 2014. The nutrient solution for ice plant, developed by Jeju National University, consisted of $Ca(NO_3)_2 \cdot 4H_2O$ 3.54g, $KNO_3$ 4.04g, $NH_4H_2PO_4$ 77g, and $MgSO_4 \cdot 7H_2O$ 2.46g in 10L (Cha et al., 2014), The nutrient solution had an EC of 1.5 $dS \cdot m^{-1}$ and was supplied to the hydroponic systems (460 mm × 300 mm× 210 mm) using a deep flow technique at a depth of 70 mm. The nutrient solutions were supplied for 10 min at one hour intervals.

The experiment was conducted in a container type plant factory (3 × 12 m), at a temperature, relative humidity, and $CO_2$ concentration of 20°C, 65%, and 400 μmol·$m^{-2}$·$s^{-1}$, respectively. The light and dark periods were 18h and 6h and the photosynthetic photon flux density (PPFD) was 150 μmol·$m^{-2}$·$s^{-1}$ during the light photoperiod. Bar-type LEDs (PGL-PFL600, Parus, Cheonan, Korea) with a 3:7 of blue (445 nm) and red (660 nm) were used as artificial light sources (30W).

***Verification of Photosynthetic Patterns of Ice Plant***

Two growth chambers of 400L (1.0m×0.8m×0.5m) each and a mixing chamber of 125L (0.5m×0.5m×0.5m)were used for the measurement of $CO_2$ absorption bu plants. Each chamber was made by acryl plates and complete-ly sealed during experimental periods. Temperatures in the chamber were maintained at 20 ºC. Air was circulated between chambers by diaphragm

pumps (Boxer 7004, Uno International Ltd., London, UK). Flow rate of the respective diaphragm pump was set to be 62Lmin$^{-1}$. $CO_2$ concentrations in the chambers were measured by using an infrared $CO_2$ sensor (LI-820, LI-COR, Lincoln, NE, USA) controlled by a data logger(CR1000, Campbell Scientific, Logan, UT, USA). The $CO_2$ concentrations were measured every 2 minutes.

Ice plants at 30days after transplanting (DAT) were used for the experiment. Actual $CO_2$ concentration in each chamber was measured during the 16h(8 and 8 for dark and light periods) at one day after the EC treatment of nutrient solutions of 1.5 dS·m$^{-1}$ (control) and 6.0 dS·m$^{-1}$ (high EC). A PPFD of 200 μmol·m$^{-2}$·s$^{-1}$ with an 8:1:1 of RBW LEDs was maintained with an initial $CO_2$ concentration of 1,750 μmol·m$^{-2}$·s$^{-1}$. Each chamber contained 24 pots of the ice plant.

***Photosynthetic Property of Ice Plant Leaves***

The net $CO_2$ assimilation rate and stomatal conductance to water vapor were measured on June 30$^{th}$ with a portable photosynthesis system (LI-6400, Li-COR, Lincoln, NE, USA) equipped with an infrared gas analyzer. Fully developed basil leaf was placed across the 6 $cm^2$ leaf chamber. The temperature and relative humidity in the leaf chamber was maintained at 25ºC and 60-70%, respectively, during measurements. The net $CO_2$ assimilation rate, as a function of the light curve, was determined at each step, every 3-4 min. PPFD ranged from 0 to 1,500 $\mu mol \cdot m^{-2} \cdot s^{-1}$ at 400 $\mu mol \cdot mol^{-1}$ of $CO_2$ concentration. Regression analyses for descriptive models were conducted for negative exponential (Evans et al., 1993; Eq. 1), non-rectangular hyperbola (Thornley, 1976; Eq. 2) models and modified non-rectangular hyperbola models (Eq. 3), as described below:

$$A = A_{max} \cdot \{(1-\exp(-\alpha \cdot I / A_{max})\} - R_d \quad \text{(Eq. II-1)}$$

$$A = [\alpha \cdot I + A_{max} - \{(\alpha \cdot I + A_{max})^2 - 4\alpha \cdot I \cdot \theta \cdot A_{max}\}^{0.5}] / 2\theta - R_d \quad \text{(Eq. II-2)}$$

$$A = [\alpha \cdot I + A_{max} - \{(\alpha \cdot I + A_{max})^2 - 4\alpha \cdot I \cdot A_{max}\}^{0.5}] / 2\theta - Rd \quad \text{(Eq. II-3)}$$

where A is the net $CO_2$ assimilation rate ($\mu mol \cdot m^{-2} \cdot s^{-1}$), $\alpha$ parameter is the initial slope, I is the photosynthetic photon flux ($\mu mol \cdot m^{-2} \cdot s^{-1}$), $A_{max}$ is the maximum net $CO_2$ assimilation rate ($\mu mol \cdot m^{-2} \cdot s^{-1}$), $\theta$ is the curvature of photosynthetic curve, and Rd is the respiration rate ($\mu mol \cdot m^{-2} \cdot s^{-1}$).

The net $CO_2$ assimilation rate as a function of the A-$C_i$ curve was determined at each step, every three to four minutes. Variable $CO_2$ concentration were maintained from photosynthetic measurement system, which resulted in $CO_2$ concentrations ranging from 100 to 1,500 $\mu mol \cdot mol^{-1}$ at a PPFD of

500 μmol·$m^{-2}$·$s^{-1}$. Sharkey's method (2007) was used to solve the parameters of biochemical models.

***Coupled Biochemical Models for Photosynthesis of Ice Plant***

Biochemical models (Eq. II-4~7) were used for acquiring the net photosynthetic rate, which is limited by the rates of $CO_2$ carboxylation by Rubisco, Ribulose 1,5-bisphophate (RuBP) regeneration, and triose phosphate utilization.

$$A = \min\{A_c,\ A_j,\ A_p\} - R_d \qquad \text{(Eq. II-4)}$$

$$A_c = V_{max}\frac{C_i - \tau^*}{C_i + K_c * (1 + \frac{O}{K_o})} \qquad \text{(Eq. II-5)}$$

$$A_j = \frac{J * (C_i - \tau^*)}{4\,(C_i + 2\,\tau^*)} \qquad \text{(Eq. II-6)}$$

$$A_p = 3 * TPU \qquad \text{(Eq. II-7)}$$

where $A_c$ is rubisco-limited photosynthetic rate, $A_j$ is RuBP regeneration limited photosynthetic rate through electron transport, $A_p$ is TPU limited photosynthetic rate, $V_{max}$ is the maximum rate of Rubisco carboxylation ($\mu mol \cdot m^{-2} \cdot s^{-1}$), $C_i$ is the intercellular $CO_2$ concentration ($\mu mol \cdot mol_{-1}$), $\tau *$ is the $CO_2$ compensation point in the absence of $R_d$ ($\mu mol \cdot mol^{-1}$), $K_c$ and $K_o$ are the Michaelis-Menten constants of Rubisco for $CO_2$ and $O_2$, respectively ($\mu mol \cdot mol^{-1}$), O is the oxygen partial pressure ($\mu mol \cdot mol^{-1}$), O is the oxygen partial pressure($\mu mol \cdot mol^{-1}$), J is the electron transport rate ($\mu mol \cdot m^{-2}\ s^{-1}$), and TPU is the triose phosphate utilization rate ($\mu mol \cdot m^{-2} \cdot s^{-1}$). The photo-

synthetic limitation parameters of the ice plant leaves were calculated by an Excel macro program developed by Sharkey (2007).

The intercellular $CO_2$ concentration ($C_i$) in the ice plant leaf was measured with a portable photosynthetic measurement system. The $C_i$ is estimated using Eq. II-8 (Caemmerer and Farquhar, 1981).

$$C_i = \frac{\left(g_{tc} - \frac{E}{2}\right) C_a - A}{g_{tc} + E/2} \qquad \text{(Eq. II-8)}$$

where $g_{tc}$ is the total conductance to $CO_2$ ($\mu mol \cdot mol^{-1}$) and E is the transpiration ($mol \cdot m^{-2}\ s^{-1}$). The stomatal conductance was described as the BWB model (Eq. II-9; Ball et al., 1987), in which the relative humidity at the leaf surface ($h_s$) is described as a linear function.

$$g_s = b + m * A\frac{h_s}{(\frac{C_s}{C_a})} \qquad \text{(Eq. II-9)}$$

where $g_s$ (mol $m^{-2} \cdot s^{-1}$) is the stomatal conductance to water vapor, b (mol$\cdot m^{-2} \cdot s^{-1}$) is the minimum stomatal conductance to water vapor at the light compensation point in the BWB model, m is the empirical coefficient for the sensitivity of $g_s$, and $C_s$ and $C_a$ are the ambient air and leaf surface $CO_2$ concentrations (μmol $mol^{-1}$). Parameters b and m were estimated by linear regression in terms of k value of $A\frac{h_s \cdot C_a}{(C_s)}$

The leaf temperature was estimated with the energy balance model as a function of $g_s$, boundary layer conductance, and environmental parameters, such as air temperature, relative humidity, and radiation (Kim and Lieth, 2003). $C_i$ and $T_L$, as well as photosynthetic active radiation (PAR), were used in the FvCB model. The net photosynthetic rate (A) and $C_i$ were used

in the BWB model. $T_L$ was estimated iteratively from the energy balance using air temperature, conductance for heat, and water vapor. Initially, $T_L$ and $C_i$ were assumed to be equal to the air temperature and $0.7C_a$, respectively, to obtain and estimate A, and then $g_s$ was obtained. $C_i$ could be estimated using A and $g_s$. These processes were conducted iteratively using the Newton-Raphson method until $C_i$ and $T_L$ became stable. The photosynthetic rates were acquired by inputting their parameters and optical characteristics of ice plant into the photosynthesis simulator (Kim and Lieth, 2003).

## RESULTS AND DISCUSSION

One day after the high EC condition, the ice plants started to absorb $CO_2$ during dark period as shown in typical CAM plants, while activated as C3 plants under normal EC condition (control) at juvenile stage (Fig II-1). During light period, all the plants activated as C3 plants. It was estimated that transition stage from C3 to CAM occurred with the accumulation of malate. Winter (1978) reported the conversion from C3 to CAM mechanism during reproductive stage occurred even though it is known as CAM plant. In this study the ice plant was proved to act as C3 plant even during juvenile in plant factory condition and therefore light and A-Ci curves for C3 plants could be used for photosynthetic analysis.

Light response curves to various light intensities were developed for ice plant leaves (Fig. II-2). The photosynthetic rate was rapidly increased at 200 $\mu mol \cdot m^{-2} \cdot s^{-1}$ PPFD and saturated at 600 $\mu mol \cdot m^{-2} \cdot s^{-1}$ PPFD. Sharp et al. (1984) reported a similar linear relationship between light intensity and photosynthetic rate at 100 $\mu mol \cdot m^{-2} \cdot s^{-1}$ PPFD.

Parameters of the negative exponential and non-rectangular hyperbola models were estimated from the regression analysis (Table II-1; Kim et al., 2003). These parameters showed C3 photosynthetic characteristics in the juvenile stage ice plants grown in the plant factory, as mentioned by Winter et al. (1978). The non-rectangular hyperbola model was more accurate, giving a value of $R^2$=0.998 for the light curve, compared with $R^2$=0.994 for the negative exponential model. The initial slope ($\alpha$) of the non-rectangular hy-

perbola was determined as 49.9mmol·mol$^{-1}$ from photosynthetic rate measurements from 0 to 100 μmol·m$^{-2}$·s$^{-1}$ PPFD. The average curvature of the non-rectangular hyperbola (Eq. II-2) for the light response curve was 0.87±0.03. The residual sum of squares between measured and predicted photosynthetic rates was lower for the non-rectangular hyperbola than for the negative exponential (not shown). The non-rectangular hyperbola gave a more accurate prediction when compared to the negative exponential; however, the negative exponential provided a simpler summary of the light response curve.

Regression analysis was conducted using the measured photosynthetic rates with increasing $CO_2$ concentration and the negative exponential model, non-rectangular hyperbola, and modified non rectangular hyperbola model

(Fig. 3). The y-axis and x-axis values of the intercept, as the estimates of $R_p$ and $C_{comp}$, respectively, were 9.3 and 117.19 $\mu mol \cdot m^{-2} \cdot s^{-1}$ (Table 2). The intercellular $CO_2$ concentrations were 63.53 and 458.53 $\mu mol \cdot m^{-2} \cdot s^{-1}$ at the compensation and saturation points and the atmospheric $CO_2$ concentrations ($C_{comp}$ and $C_{sat}$) were 117.19 and 632.91 $\mu mol \cdot m^{-2} \cdot s^{-1}$, respectively and negative exponential model's accuracy was highest among regression curves (Table 2). The photosynthetic limitation curve for ice plant (Fig. 3) was obtained using an Excel macro program (Sharkey et al, 2007). The photosynthetic rates were determined using a Rubisco carboxylation rate for range intercellular $CO_2$ concentrations ranging from 100 to 150 $\mu mol \cdot mol^{-1}$, a Ribulose 1,5-bisphosphate (RuBP) regeneration rate ranging from 150 to 250 $\mu mol \cdot mol^{-1}$, and the triose phosphate utilization rate (TPU) ranging

from 250 to 800 μmol·mol$^{-1}$. The photosynthetic A-Ci curve of the ice plant was concluded to fit the parameters of Sharkey's method.

The maximum carboxylation rate ($V_{max}$, μmol·m$^{-2}$·s$^{-1}$), the maximum rate of electron transport ($J_{max}$, μmol·m$^{-2}$·s$^{-1}$), the TPU (μmol·m$^{-2}$·s$^{-1}$), and the mitochondrial respiration in the light ($R_d$, μmol·m$^{-2}$·s$^{-1}$) were 222.3, 234.9, 13.0, and 6.25, respectively (Table II-3). These parameters for ice plant were in the range of parameter values calculated for roses by Kim and Lieth (2003). The parameters of minimum stomatal conductance to water vapor at the light compensation point (b) and the empirical coefficient (m) for the sensitivity of $g_s$ to A, $C_s$, and $h_s$ in the BWB were solved with linear regression analysis using the measured A-Ci values (Fig. II-3). The parameter of the m value showing the stomatal conductance slope was lower than that

published for roses, so the A-$C_i$ curves should be acquired according to various environmental conditions.

The parameters of minimum stomatal conductance at the light compensation point (b) with the empirical coefficient (m) for the sensitivity of $g_s$ to A, $C_s$, and $h_s$ in the BWB model were solved as 0.0487 and 0.0012 by the linear regression analysis using the measured A-$C_i$ values (Fig. II-4). The stomatal conductance slope (m) for ice plant was lower than that reported for roses. The k value (Eq. II-10) showed a weak linearity with the stomatal conductance shown in Fig. II-5, as reported by Ball et al (1987).

$$k = A\frac{h_s C_a}{C_s} \qquad \text{(Eq. II-10)}$$

The residual sum of squares between measured and predicted photosynthetic rates in the coupled biochemical model was larger than that obtained with the negative exponential model (Table II-4). The biochemical model underestimated the photosynthetic rate when compared to the negative exponential model at a high concentration of $CO_2$. However, the coupled biochemical model using temperature, $CO_2$, and stomatal conductance, was very effective for analyzing the photosynthetic rate during the juvenile stage. From this experiment, we confirmed that the ice plant was converted from C3 to CAM under a stressed condition like EC 6.0dS·m$^{-1}$. Therefore, even though the ice plant is a CAM plant, the A-Ci and light curves indicated that performs $C_3$ photosynthesis during the juvenile stage in plant factory conditions.

Table II-1. Photosynthetic parameters of the negative exponential (Eq. II-1), non-rectangular hyperbola (Eq. II-2), and modified nonrectangular hyperbola (Eq. II-3) models calculated from the light response curves obtained for ice plant in Fig. II-2.

| Parameter | Negative exponential model ($R^2$=0.994) | Non-rectangular hyperbola ($R^2$=0.998) | Modified non-rectangular Hyperbola ($R^2$=0.985) |
|---|---|---|---|
| $A_{max}$ ($\mu mol \cdot m^{-2} \cdot s^{-1}$)[z] | 21.4±2.61[t] | 24.5±0.31[u] | 28.3±0.60 |
| $\alpha$ ($mmol \cdot mol^{-1}$)[y] | 71.8±1.12 | 49.9±0.46 | 49.9±0.46 |
| $\theta$[x] | - | 0.9±0.03 | 1.3±0.06 |
| $R_d$ ($\mu mol \cdot m^{-2} \cdot s^{-1}$)[x] | 3.4±0.09 | 2.8±0.24 | 2.18±0.08 |
| $L_{comp}$ ($\mu mol \cdot m^{-2} \cdot s^{-1}$)[w] | 50.4±0.42 | 55.9±3.95 | 56.0±2.25 |
| $L_{sat}$ ($\mu mol \cdot m^{-2} \cdot s^{-1}$)[v] | 496.0±23.21. | 490.9±23.4 | 569.5±11.72 |

[z]Maximum photosynthetic capacity; [y]Apparent quantum yield; [x]Curvature of curve; [w]Dark respiration rate.

[v]Light compensation point; [u]Light saturation point; [t]Mean ± standard error (n=3).

Table II-2. Photosynthetic parameters of the negative exponential model (Eq. II-1), non-rectangular hyperbola (Eq. II-2), and modified nonrectangular hyperbola (Eq. II-3) models calculated from the A-Ci curves obtained for ice plant in Fig. II-3.

| Parameters | Negative exponential ($R^2$=0.994) | Non-rectangular hyperbola ($R^2$=0.986) | Modified non-rectangular hyperbola ($R^2$=0.975) |
|---|---|---|---|
| $A_{max}$ ($\mu mol \cdot m^{-2} \cdot s^{-1}$)[z] | 39.5±1.05[u] | 44.2±3.10 | 36.4±0.70 |
| $\alpha$ ($mmol \cdot mol^{-1}$)[y] | 163.8±16.55 | 98.9±0.01 | 98.9±0.01 |
| $\theta$[x] | - | 0.9±0.04 | 0.8±0.06 |
| $R_d$ ($\mu mol \cdot m^{-2} \cdot s^{-1}$)[w] | 9.3±1.36 | 5.1±0.78 | 2.2±0.09 |
| $C_{comp}$ ($\mu mol \cdot mol^{-1}$)[v] | 117.2±0.57 | 58.3±2.94 | 51.3±2.52 |
| $C_{sat}$ ($\mu mol \cdot mol^{-1}$)[u] | 632.9±39.62 | 516.1±32.80 | 502.8±10.27 |

[z]Maximum photosynthetic capacity; [y]Apparent quantum yield; [x]Curvature of curve; [x]Dark respiration rate.

[w]$CO_2$ compensation point; [v]$CO_2$ saturation point; [u]Mean ± standard error (n=3).

Table II- 3. Estimated photosynthetic parameters of the biochemical model for ice plant at a leaf temperature of 24.8°C.

| Parameter | $V_{max}$[z] ($\mu mol \cdot m^{-2} \cdot s^{-1}$) | $J_{max}$[y] ($\mu mol \cdot m^{-2} \cdot s^{-1}$) | TPU[x] ($\mu mol \cdot m^{-2} \cdot s^{-1}$) | $R_d$[w] ($\mu mol \cdot m^{-2} \cdot s^{-1}$) |
|---|---|---|---|---|
| Value | 222.3±1.53[t] | 234.9±1.25 | 13.0±0.23 | 6.25±0.163 |

[z]Maximum carboxylation rate; [y]Maximum rate of electron transport; [x]Triose phosphate utilization rate

[w]Mitochondrial respiration in the light; [v]Minimum stomatal conductance to water vapor at the light

[u]Empirical coefficient for the sensitivity of $g_s$ to A, $C_s$ and $h_s$ in the BWB model

[t]Mean ± standard error (n=3).

Table II-4. Comparison of photosynthetic rate and residual sum of squares among negative exponential, non-rectangular hyperbola, modified non-rectangular hyperbola, and biochemical models for ice plant.

| $Ci^z$ ($\mu mol \cdot mol^{-1}$) | Measured value ($\mu mol\ m^{-2}\ s^{-1}$) | Predicted value ($\mu mol\ m^{-2}\ s^{-1}$) | | | |
|---|---|---|---|---|---|
| | | Negative Exponential | Non-rectangular hyperbola | Modified non-rectangular hyperbola | Biochemical |
| 84 | 1.86 | 2.57 | 2.31 | 2.95 | 3.02 |
| 142 | 6.70 | 8.91 | 7.19 | 8.44 | 10.84 |
| 187 | 9.98 | 12.99 | 10.84 | 12.69 | 16.27 |
| 249 | 20.77 | 17.63 | 15.65 | 18.55 | 20.03 |
| 452 | 28.93 | 27.25 | 27.92 | 37.74 | 25.87 |
| 603 | 31.87 | 31.00 | 32.54 | 42.05 | 27.69 |
| Residual sum of squares | - | 27.82 | 28.81 | 197.72 | 85.29 |

[z]Intercellular $CO_2$ concentration.

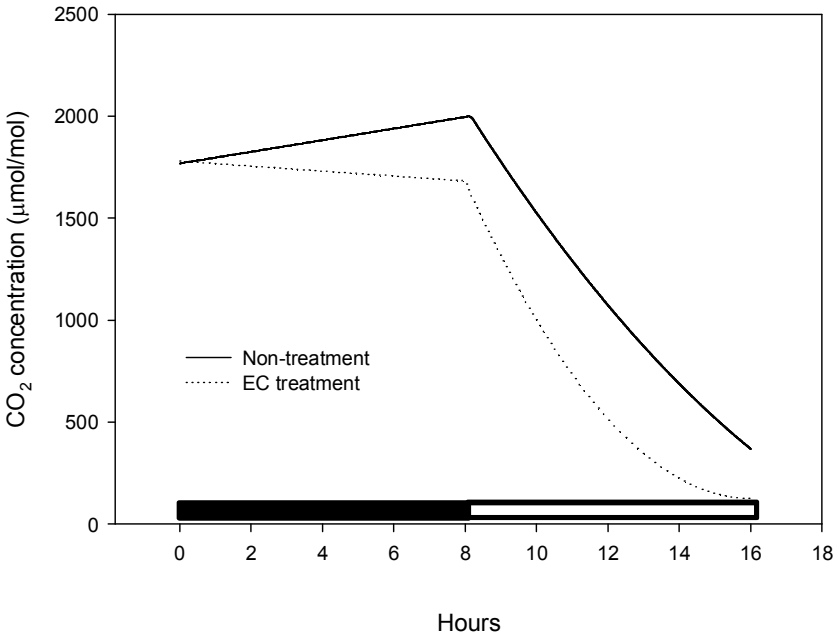


Fig. II-1. Change in $CO_2$ concentration in growth chamber during the 16 h (8 h and 8h for dark and light periods). Measurement of the $CO_2$ concentration started from one day after electrical conductivity (EC) treatments of nutrient solutions at 1.5 $dS \cdot m^{-1}$ (control, solid-line) and 6.0 $dS \cdot m^{-1}$ (high EC, dotted-line). Each chamber contains 24 pots of ice plant.

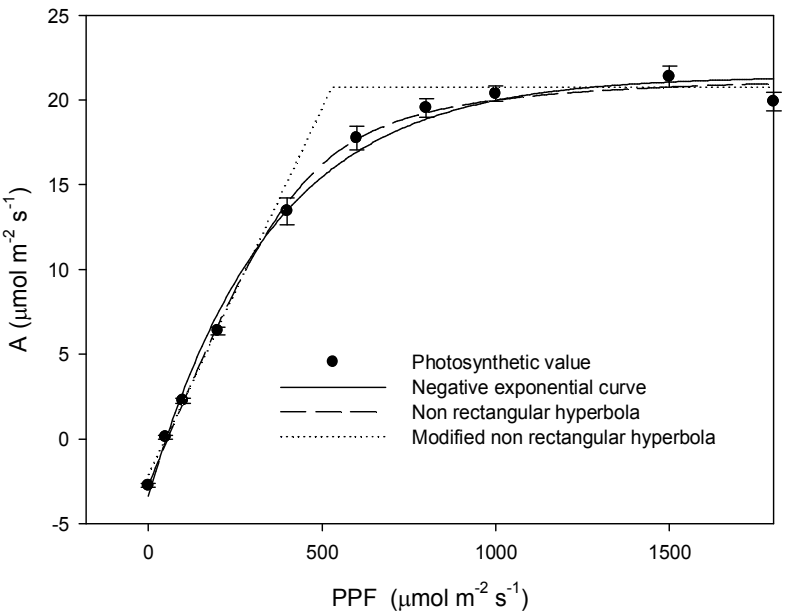


Fig. II-2. Regression response curves for light in ice plant leaves using negative exponential, non-rectangular hyperbola, and modified non-rectangular models at a $CO_2$ concentration of 400 μmol·mol$^{-1}$ for ice plant leaves. Vertical bars are the standard errors of the means from three replications. A and PPFD are the $CO_2$ assimilation rate and the photosynthetic photon flux, respectively.

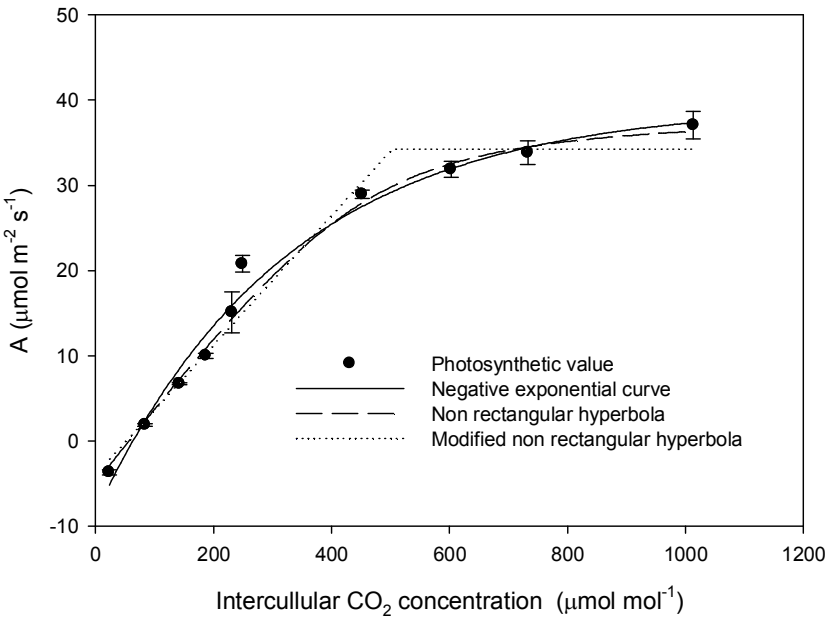


Fig. II-3. Net $CO_2$ assimilation rate (A) as a function of the intercellular $CO_2$ concentration in ice plant leaves using negative exponential, non-rectangular hyperbola, and modified non-rectangular models at a photosynthetic photon flux of 500 $\mu mol \cdot m^{-2} \cdot s^{-1}$. Vertical bars are the standard errors of the means from three replications.

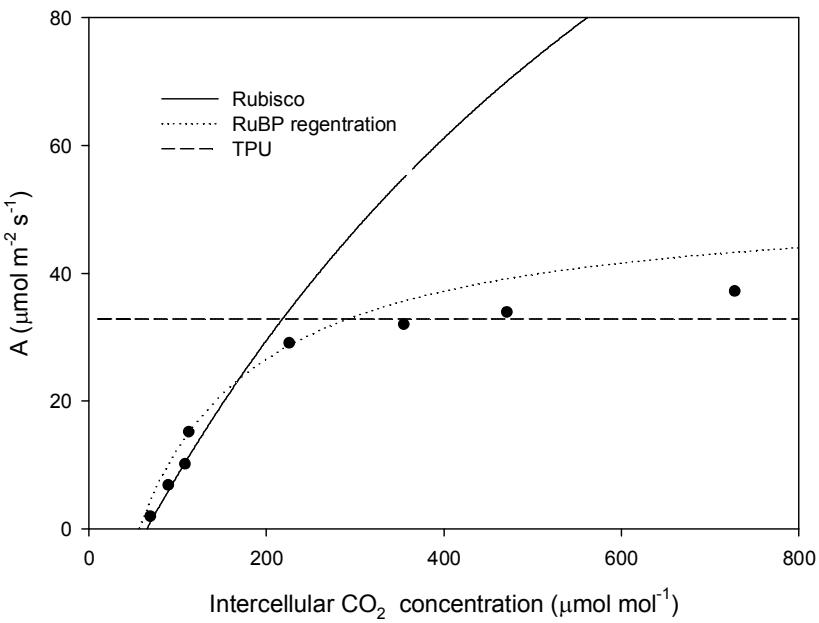


Fig. II-4. Net $CO_2$ assimilation rate (A) as a function of intercellular $CO_2$ concentration in ice plant leaves at a photosynthetic photon flux of 500 $\mu mol \cdot m^{-2} \cdot s^{-1}$. Rubisco, RuBP, or TPU limitations are assumed for prediction of photosynthesis.

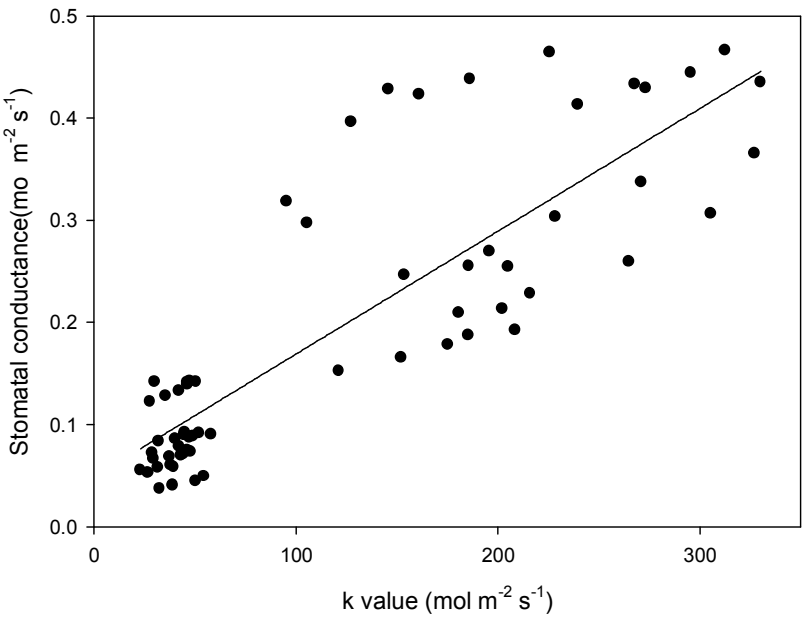


Fig. II-5. Relationship between stomatal conductance ($g_s$) and k value (=A· $h_s$ · $C_a$ / $C_s$) ($R^2$=0.8467). The values of b and m in Eq. 8 were acquired as 0.0487 and 0.0012 with this result under temperature conditions ranging from 20 to 35℃. A, $h_s$, $C_a$, and $C_s$ are the net photosynthetic rate, relative humidity of the leaf surface, ambient $CO_2$ partial pressure, and $CO_2$ partial pressure at the leaf surface, respectively.

.

## LITERATURE CITED

Ball, J.T., I.E. Woodrow, and J.A. Berry. 1987. A model predicting stomatal conductance and its contribution to the control of photosynthesis under different environmental conditions, p. 221-224. In: Biggins J(ed). Progress Photosyn. Res. Martinus Nijhoff publishers, The Netherlads.

Caemmerer, S.V. and G.D. Farquhar. 1981. Some relationships between the biochemistry of photosynthesis and the gas exchange of leaves. Planta 153:376-387.

Cha, M.K., J.S. Kim, H.J. Shin, J.E. Son, and Y.Y. Son. 2014. Practical design of an artificial light-used plant factory for common ice plant (*Mesembryanthemum crystallinum* L.). Protected Hort. Plant Factory 23:371-375.

Cushman, J.C. 2001. Crassulacean acid metabolism: a plastic photosynthetic adaptation to arid environments. Plant Physiology 127:1439-1448.

Evans, J.R., I. Jakobsen, and E. Orgren. 1993. Photosynthetic light-response curves. 2. Gradients of light absorption and photosynthetic capacity. Planta 189:191-200.

Harley, P.C., R.B. Thomas, J.F. Reynolds, and B.R. Strain. 1992. Modeling

photosynthesis of cotton grown in elevated $CO_2$. Plant Cell Environ. 23: 351-363.

Heuvelink, E. 1999. Evaluation of a dynamic simulation model for tomato crop growth a development. Ann. Bot. 83: 413-422.

Kim, P.G., K.Y. Lee, S.D. Hur, S.H. Kim, and E.J. Lee. 2003. Effects of shading treatment on photosynthetic activity of *Acanthopanax senticosus*. Kor. J. Ecol. 26: 321-326.

Kim, S.H. and J.H. Lieth. 2003. A coupled model of photosynthesis, stomatal conductance and traspiration for a rose leaf (*Rosa hybrida* L.). Ann. Bot. 91: 771-781.

Leuning, R. 1995. A critical appraisal of a combined stomatal-photosynthesis model. Plant Cell Environ. 18:339-355.

Medlyn, B.E., F.W. Badeck, D.G. G. de Pury, C.V.M. Barton, and M. Broadmeadow. 1999. Effects of elevated $CO_2$ on photosynthesis in European forest species: a meta-analysis of model parameters. Plant Cell Environ. 22: 1475-1495.

Nikolov, N.T., W.J. Massman, and A.W. Shoettle. 1995. Coupling biochemical and biophysical processes at the leaf level: an equilibrium photosynthesis model for leaves of C3 plants. Ecol. Modelling 80:205-235.

Sharkey, T.D., C. J. Bernacchi, G.D. Farquhar, and E.L. Sinsaas. 2007. Fitting photosynthetic carbon dioxide response curves for C3 leaves. Plant Cell Environ.30:1035-1040.

Sharp, R.E., M.A. Mattews, and J.J. Boyer. 1984. Kok effect and the quantum yield of photosynthesis. Plant Physiol 75:95-101.

Thornley, J. H.M. 1976. Mathematical models. Plant physiology, Academic Press. London, 318p

Winter, K., U. Ltittge, and E. Winter. 1978. Seasonal shift from C3 photosynthesis to crassulacean acid metabolism in *Mesembryanthemum crystallinum* growing in its natural environment. Oecologi 34:225-237.

# Chapter III

## GROWTH MODELLING OF SWEET BASIL AND ICE PLANT USING EXPO-LINEAR FUNCTIONS IN PLANT FACTORIES


### ABSTRACT

Sweet basil is a year-round popular item among herbal species and the ice plant, a medicinal plant with well-known retarding effects on diabetes mellitus, is increasingly being produced in plant factories. The objectives of this study were to find out environmental set-point such as temperature and $CO_2$ concentration of sweet basil and ice plant for plant factory operation and to make growth models for ice plant and sweet basil using expo-linear functional equations in a closed-type plant production system. The growth models fir temperature and $CO_2$ concentration were developed by using an expo-

linear model. The adequate air temperatures and $CO_2$ concentration for sweet basil were 25°C and 800 μmol·mol$^{-1}$, respectively, considering harvesting period, leaf fresh weight and leaf area. Then, the relative growth rates are 0.1 g·g$^{-1}$·d$^{-1}$ in 25°C of air temperature and 2.63 g·g$^{-1}$·d$^{-1}$ in 800 μmol·mol$^{-1}$ of $CO_2$ concentration. Also the adequate temperatures and $CO_2$ concentration were 25°C and 800 μmol·mol$^{-1}$, respectively, considering harvesting period, leaf fresh weight, leaf area of ice plant, and $CO_2$ leakage. Its relative growth rates were 0.15 in 25°C of air temperature and 0.52 g·g$^{-1}$·d$^{-1}$ in 800 μmol·mol$^{-1}$ of $CO_2$ concentration.

*Keywords:* $CO_2$ concentration, expo-linear function, light use efficiency, *Mesembryanthemum crystallinum* L., *Ocimum basilicum* L., temperature.

# INTRODUCTION

The cultivation and utilization of herb with high-quality are increasing with income improvement and home demand for herb. Particularly, consumers have high preference for herb production under plant factory as aspect of utilization in utilizing of fresh herb (Yeo, 2004). Sweet basil (*Ocimum basilicum* L.) is year-round popular item among herbal crops (Tesi, 1995). Especially, the urgent demand of fresh sweet basil stimulates its cultivation under plant factory. And the ice plant (*Mesembryanthemum crystallinum* L.), a member of the *Aizoaceae* family, synthesizes a polyol in the leaf that imparts antioxidant properties, making this plant increasingly attractive for plant factory production. Sweet basil and ice plant are proper for production of plant factory owing to high price and medicinal effect. Sweet basil and ice plant are spreading in the on-line market as similar price with comparison to fresh ginseng.

A factory-style plant production system can make year-round and planned production with yield and quality control of crops by using environmental control. The environments such as light, temperature, relative humidity, and $CO_2$ concentration could be controlled as proper levels in condition of crop production (Cha et al., 2014) and the prediction of growth is easier in closed-type plant production than in greenhouse. Expo-linear function is often used for the prediction of crop production (Goudriaan and Monteith, 1990).

Highly-developed plant factories have characteristics of continuous production, rapid production, and high energy consumption. Required key points to spread commercial plant factories are to find set points of light, temperature and $CO_2$ to maximize the photosynthesis on economic aspect and to select proper crops for plant factory production. Thorney (2000) described the photosynthesis rate of canopy considering leaf area index, light

extinction coefficient, and temperature with Taylor series. To find properly environmental set points, it is necessary to make growth models of sweet basil and ice plant. Especially, temperature has a close relationship with respiration and growth rate (Thonrey, 1977) and 49% of $CO_2$ could be absorbed into crops at 1000 $\mu mol \cdot mol^{-1}$ under unventilated greenhouse (Kuroyanagi, 2014).

It is necessary for developing their modellings of growth under plant factory owing to the prediction of harvest and the maximization of production and profit of plant factory. The growth modellings of sweet basil and ice plant under plant factory environments were not accomplished so far.

The objectives of this study were to find out adequate set-point of temperature and $CO_2$ concentration for sweet basil and ice plant in plant factories and to develop their growth model.

## MATERIALS AND METHODS

### *Plant Materials and Cultivation Conditions*

Sweet basil and ice plant seed (Asia seed, Seoul, Korea) was sown on rock-wool seed board (60 cm x 40 cm) at April 30$^{th}$ and Nov. 5$^{th}$ of 2014 for $CO_2$ concentration and temperature experiment in venlo-type greenhouse of protected horticulture research institute. The planting dates are May 14th and Nov. 26th for sweet basil and May 22nd and Dec. 1st, and their seedling with three to four leaf was planted on planting board of polystyrene (Thickness 30 mm, 10 cm × 10 cm density). The nutrient solution composition for sweet basil developed by the University of Seoul was $Ca(NO_3)_2 \cdot 4H_2O$ 6.8 g, $KNO_3$ 5.9 g, $NH_4H_2PO_4$ 1.4 g, and $MgSO_4 \cdot 7H_2O$ 3.7 g in 10 L (Yeo and Lee, 2014). The nutrient solution for ice plant, developed by Jeju National University, consisted of $Ca(NO_3)_2 \cdot 4H_2O$ 3.5 g, $KNO_3$ 4.0 g, $NH_4H_2PO_4$ 77.0 g, and $MgSO_4 \cdot 7H_2O$ 2.5 g in 10L (Cha et al., 2014), The

nutrient solution had an EC of 1.5 $dS \cdot m^{-1}$ and was continuously supplied to the hydroponic systems (460 mm × 300 mm× 210 mm) using a deep flow technique at a depth of 70 mm. The height of nutrient solution tank is 140 mm and submerged pump supply nutrient solution to cultivation bed in hydroponic system. The nutrient solution was supplied for 10 minutes at one hour interval. The experiment was accomplished in container-type plant factory (3 m × 12 m) of protected horticulture research institute, national institute of horticultural and herbal science. The experiment was conducted in a plant factory (3 m × 12 m), at a temperature, relative humidity, and $CO_2$ concentration of 20.0±1.0°C, 65±15%, and 500±50 $\mu mol \cdot mol^{-1}$, respectively. The light/dark period was 18h/6h and the photosynthetic photon flux density (PPFD) was 150±20 $\mu mol \cdot m^{-2} \cdot s^{-1}$ during the light period. Bar-type LEDs (PGL-PFL600, Parus, Cheonan, Korea) with a 3:7 mixture of blue (445 nm) and red (660 nm) were used as artificial light sources. The total

leaf areas for each plant were measured using a LI-3100 leaf area meter (Li-Cor, Lincoln, NE, USA). The number of leaves, shoot fresh weight, and shoot dry weight were also measured. The shoot fresh weight was determined immediately after harvest, and the shoot dry weight was determined after harvest, and the shoot dry weight was determined after oven drying at 70℃ for 72 h.

***Temperature and $CO_2$ Treatments Experiment for Sweet Basil and Ice Plant***

Inside set points of the container-type plant factory were separately set as 15, 20, 25, and 30℃ for temperature and 500, 800, 1,000, and 1,500 $\mu mol \cdot mol^{-1}$ for $CO_2$ concentrations, respectively. The temperature and $CO_2$ concentration were managed with heater /cooler and liquid $CO_2$ supplier controlled by a data logger (CR-1000, Campbell, USA). After transplanting,

plant height, number of leaves, leaf area, fresh weight of leaf and stem, and their dry weight of sweet basil and ice plant were analyzed at about 10 days interval. 20 W LED lamps of bar type (were used for artificial lighting. The lamp consist of a 3:7 mixture of 2W blue (445nm peak) and red (660nm peak) LED.

***Growth Model and Statistical Analysis***

An expo-linear equation, expressing the shoot dry weight as a function of time, were used (Goudriaan and Monteith,1990):

$$W=C_m/R_m \cdot \ln[1+\exp\{R_m \cdot (t-t_b)\}] \quad \text{(Eq. III-1)}$$

where W is the biomass (shoot dry weight, $g \cdot m^{-2}$), $C_m$ is the maximum crop growth rate ($g \cdot m^{-2} \cdot d^{-1}$), $R_m$ is the relative growth rate ($g \cdot g^{-1} \cdot d^{-1}$) in the exponential growth phase, t is the time after transplanting (day), and $t_b$ is the time at which the crop effectively reaches a linear phase of growth (lost time, d).

A completely randomized block design was used under three blocks per treatment with five plant replications per block. The data was analyzed with the statistical analysis program SAS (SAS Institute, Cary, NC, USA). The variables were estimated using the Gauss-Newton algorithm, a nonlinear least squares technique.

## RESULTS AND DISCUSSION

The temperatures and $CO_2$ concentrations in the container-type plant factory could be well controlled within 1.1°C and 37 μmol·mol$^{-1}$(Table III-1). The growth of sweet basil was adequate 20 and 25°C in terms of dry matter, and (Fig. III-1) and the fresh weight and leaf area were the highest 25°C (Table III-3).

The expo-linear formula suggested by Goudriaan (1978) could easily be determined the relation between crop growth rate and relative growth rate. The nonlinear regression procedure of SAS (v9.1) could obtain the parameters of the expo-linear equation of the response of temperature for sweet basil. The R square value for expo-linear regression was 0.99 and the crop growth rate at 20°C was the highest (Table III-2).

The growth of ice plant was adequate at an inside temperature of 25°Cconsidering fresh weight and leaf weight (Table. III-4). And the response curves of dry matter could be obtained by the regression of expo-linear function (Table III-3). Each R square value in the regressed expo-linear model could be mostly explained over 78%by temperature response.. Non-linear regression procedure of SAS could show the expo-linear regression of the response of temperature for ice plant. The R square value for expo-linear regression for ice plant was lower at the temperatures of 15 and 25℃ than at those of 20 and 30℃.

The growth of sweet basil was adequate at a $CO_2$ concentration of 800 μmol $mol^{-1}$ considering dry matter, harvesting period, and $CO_2$ leakage (Fig. III-3, Tables III-6 and 7). Each R square value of regressed expo-linear

model could be mostly explained over 99% by $CO_2$ response. The relative growth rate was 2.63 $g \cdot g^{-1} \cdot d^{-1}$ at a $CO_2$ concentration of 800 $\mu mol \cdot mol^{-1}$ (Table III-6). The growth of ice plant was adequate at a $CO_2$ concentration of 800 $\mu mol\ mol^{-1}$ considering harvesting period, leaf fresh weight, leaf area of ice plant, and $CO_2$ leakage (Tables III-8 and 9). The relative growth rate was 0.52 $g \cdot g^{-1} \cdot d^{-1}$ at a $CO_2$ concentration of 800 $\mu mol \cdot mol^{-1}$ (Table III-8).

Table III-1. Set and measured values of temperature and $CO_2$ concentration for sweet basil and ice plant.

| | | | | | |
|---|---|---|---|---|---|
| Temperature (°C) | Set value | 15 | 20 | 25 | 30 |
| | Measured | 15.4±0.43[z] | 20.2±0.51 | 25.1±0.61 | 29.9±1.13 |
| $CO_2$ concentration ($\mu mol \cdot mol^{-1}$) | Set value | 500 | 800 | 1000 | 1500 |
| | Measured | 533.9±2.12[z] | 767.4±4.43 | 1021.5±7.41 | 1505.1±6.43 |

[z]Mean±SE.

Table III-2. The square of R and parameters of regressed expo-linear function at different temperatures for sweet basil.

| Expo-linear function[z] | $f=C_m/R_m \cdot \ln[1+\exp\{R_m \cdot (x-t_b)\}]$ | | | |
|---|---|---|---|---|
| Parameter | 15 | 20 | 25 | 30 |
| $R^2$ | 0.99 | 0.99 | 0.99 | 0.99 |
| $C_m$ | 4.84 | 12.49 | 11.01 | 5.07 |
| $R_m$ | 0.13 | 0.09 | 0.10 | 1.33 |
| $t_b$ | 11.93 | 28.37 | 25.36 | 5.60 |

[z]$C_m$: crop growth rate($g \cdot m^{-2} \cdot d^{-1}$), $R_m$: relative growth rate ($g \cdot g^{-1} \cdot d^{-1}$), x: days after planting (d), $t_b$: the start moment of the linear phase (d).

Table III-3. Effect of temperature on plant height, number of leaves, leaf area, and leaf fresh weight of sweet basil at 43 days after planting.

| Temperature ($^{o}$C) | Plant height (mm/plant)[z] | Number of leaves (/plant) | Leaf area ($cm^2$/plant) | Leaf fresh weight (g/plant) |
|---|---|---|---|---|
| 15 | 190.7 b | 12.0 b | 230.8 c | 3.57 b |
| 20 | 296.7 a | 14.0 ab | 422.0 ab | 8.03 a |
| 25 | 300.0 a | 16.0 a | 493.4 a | 8.97 a |
| 30 | 348.3 a | 16.7 b | 327.7 bc | 9.20 a |

[z]Mean separation within columns according to LSD test at 5% significance level.

Table III-4. The square of R and parameters of regressed expo-linear function at different temperatures for ice plant.

| Expo-linear function[z] | $f=C_m/R_m \cdot \ln[1+\exp\{R_m \cdot (x-t_b)\}]$ | | | |
|---|---|---|---|---|
| Temperature ($^oC$) | 15 | 20 | 25 | 30 |
| $R^2$ | 0.99[y] | 0.99 | 0.79 | 0.99 |
| $C_m$ | 20.21 | 23.38 | 23.89 | 28.0 |
| $R_m$ | 0.181 | 0.200 | 0.150 | 0.164 |
| $t_b$ | 36.38 | 34.99 | 42.22 | 39.13 |

[z]f: dry matter ($g \cdot m^{-2}$), $C_m$: crop growth rate($g \cdot m^{-2} \cdot d^{-1}$), $R_m$: relative growth rate ($g \cdot g^{-1} \cdot d^{-1}$),

x: days after planting (d), $t_b$: the start moment of the linear phase (d).

Table III-5. Effect of temperature on number of leaves, leaf area, and leaf fresh weight of ice plant at 44 days after planting.

| Temperature (°C) | No. of leaves (/plant)[z] | Leaf area ($cm^2$/plant) | Leaf fresh weight (g/plant) |
|---|---|---|---|
| 15℃ | 9.3 c | 172.1 c | 28.6 b |
| 20℃ | 12.0 ab | 322.9 b | 50.1 a |
| 25℃ | 13.3 a | 399.9 a | 58.0 a |
| 30℃ | 11.3 b | 323.4 b | 51.4 a |

[z]p=0.05 (LSD test)

Table III-6. The square of R and parameters of regressed expo-linear function at different $CO_2$ concentrations for sweet basil.

| Expo-linear function[z] | $f=C_m/R_m \cdot \ln[1+\exp\{R_m \cdot (x-t_b)\}]$ | | | |
|---|---|---|---|---|
| $CO_2$ concentration (umol $mol^{-1}$) | 500 | 800 | 1000 | 1500 |
| $R^2$ | 0.99[y] | 0.99 | 0.99 | 0.99 |
| $C_m$ | 30.80 | 4.66 | 6.66 | 6.71 |
| $R_m$ | 0.075 | 2.629 | 0.141 | 0.167 |
| $t_b$ | 48.74 | 4.32 | 13.59 | 11.94 |

[z]f: dry matter ($g \cdot m^{-2}$), $C_m$: crop growth rate($g \cdot m^{-2} \cdot d^{-1}$), $R_m$: relative growth rate ($g \cdot g^{-1} \cdot d^{-1}$),

x: days after planting (d), $t_b$: the start moment of the linear phase (d).

Table III-7. Effects of $CO_2$ concentration on number of leaves, leaf area, and leaf fresh weight of sweet basil at 43 days after planting.

| $CO_2$ concentration ($\mu mol\ mol^{-1}$) | Plant height (mm/plant)[z] | Number of leaves (/plant) | Leaf area ($cm^2$/plant) | Leaf fresh weight (g/plant) |
|---|---|---|---|---|
| 500 | 164.0 b | 31.0 a | 307.4 b | 13.69 b |
| 800 | 239.3 ab | 22.0 b | 238.9 b | 10.39 b |
| 1000 | 259.0 a | 28.0 a | 242.5 b | 10.33 b |
| 1500 | 228.3 ab | 24.0 b | 484.7 a | 18.55 a |

[z]Mean separation within columns according to LSD test at 5% significance level.

Table III-8. The square of R and parameters of regressed expo-linear function at different $CO_2$ concentrations for ice plant.

| Expo-linear function[z] | $f=C_m/R_m \cdot \ln[1+\exp\{R_m \cdot (x-t_b)\}]$ | | | |
|---|---|---|---|---|
| $CO_2$ concentration ($\mu mol\ mol^{-1}$) | 500 | 800 | 1000 | 1500 |
| $R^2$ | 0.99 | 0.99 | 0.99 | 0.99 |
| $C_m$ | 3.00 | 18.01 | 13.71 | 7.75 |
| $R_m$ | 1.011 | 0.521 | 1.836 | 2.004 |
| $t_b$ | 10.02 | 20.32 | 18.04 | 15.54 |

[z]f: dry matter ($g \cdot m^{-2}$), $C_m$: crop growth rate($g \cdot m^{-2} \cdot d^{-1}$), $R_m$: relative growth rate ($g \cdot g^{-1} \cdot d^{-1}$), x: days after planting (d), $t_b$: the start moment of the linear phase (d).

[y]$p<0.01$(LSD test).

Table III-9. Effect of $CO_2$ concentration on number of leaves, leaf area, and leaf fresh weight of ice plant at 44 days after planting.

| $CO_2$ concentration ($\mu mol\ mol^{-1}$) | Number of leaves (/plant)[z] | Leaf area ($cm^2$/plant) | Leaf fresh weight (g/plant) |
|---|---|---|---|
| 500 | 17.3 b | 115.7 c | 22.71 c |
| 800 | 25.7 a | 476.7 a | 78.15 a |
| 1000 | 20.0 ab | 231.3 b | 38.55 b |
| 1500 | 20.0 ab | 115.8 c | 19.01 c |

[z]p=0.05 (LSD test).

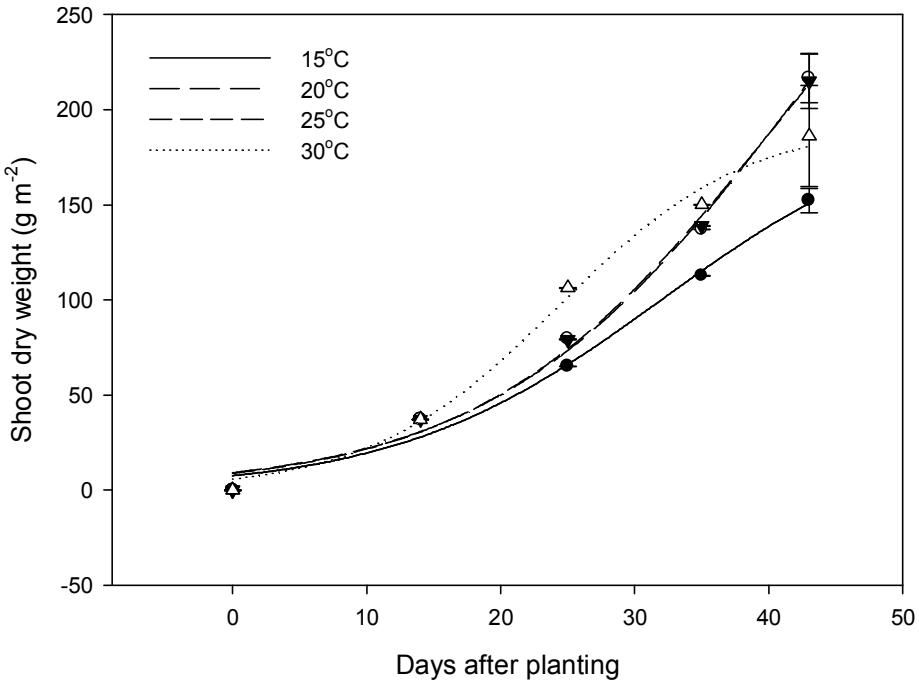


Fig. III-1. Change in shoot dry weight of sweet basil with days after planting according to temperature. Vertical bar is standard error.

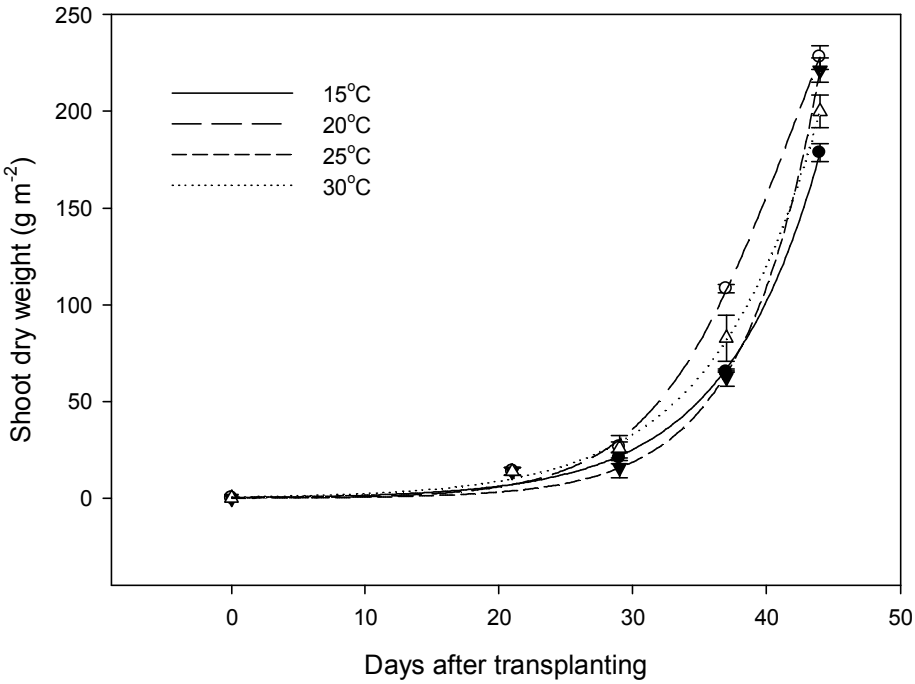


Fig. III-2. Change in shoot dry weight for ice plant with days after planting according to temperature. Vertical bar is standard error.

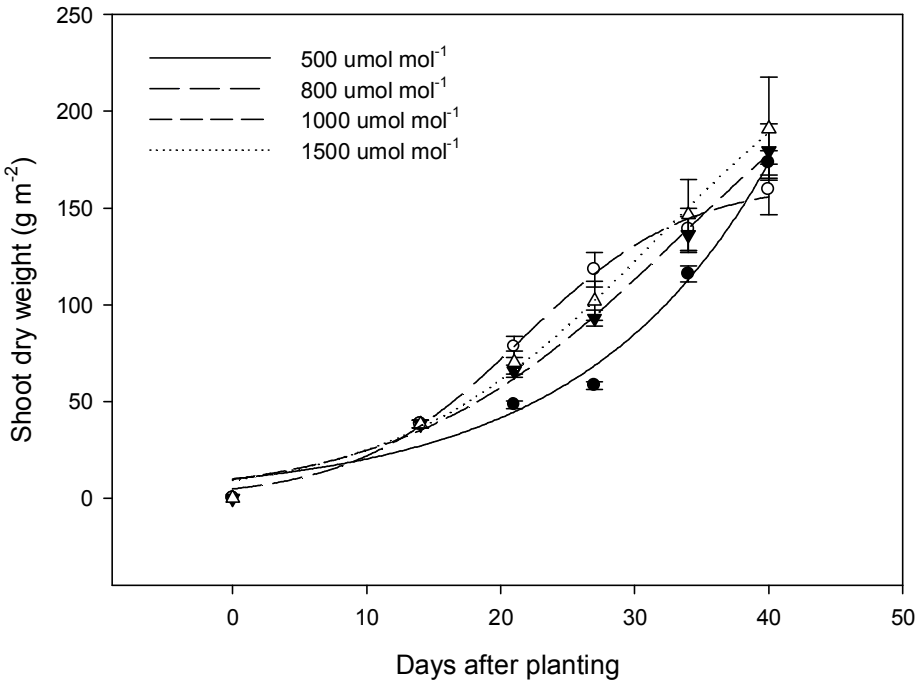


Fig. III-3. Change in shoot dry weight of sweet basil with days after planting according to $CO_2$ (umol $mol^{-1}$) concentration. Vertical bar is standard error.

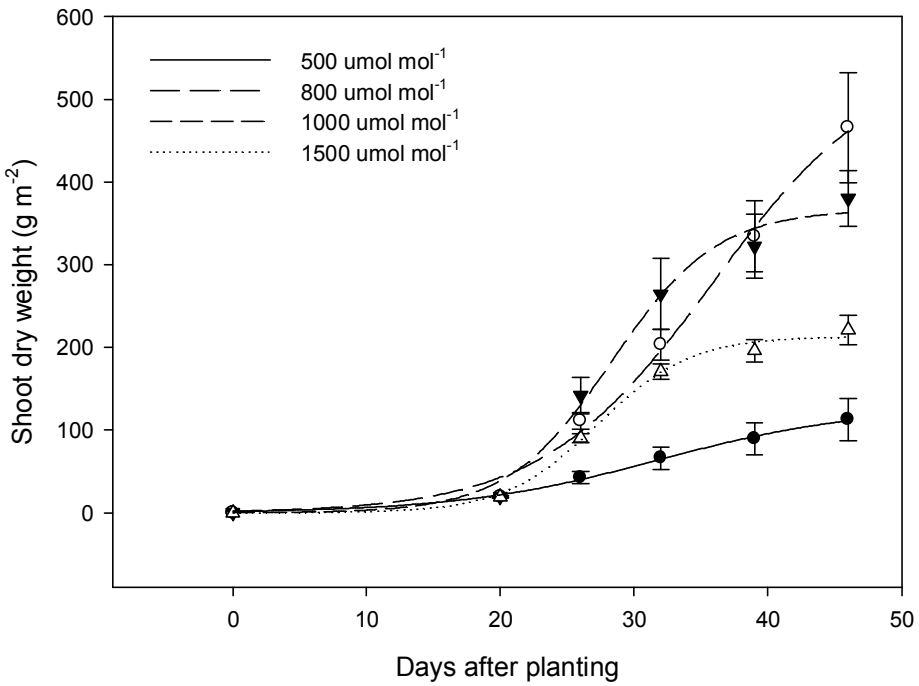


Fig. III-4. Change in shoot dry weight for ice plant with days after planting according to $CO_2$ (umol $mol^{-1}$) concentration. Vertical bar is standard error.

## LITERATURE CITED

Cha, M.K., J.S. Kim, H.J. Shin, J.E. Son, and Y.Y. Son. 2014. Practical design of an artificial light-used plant factory for common ice plant. Protec. Hort. Plant Factory 23: 371-375.

Cho, Y.Y., J.H. Lee, J.H. Shin, and J.E. Son. 2015. Development of an expolinear growth model for pak-choi using the radation intergral and planting density. Hort. Environ. Biotechnol. 56:310-315.

Christopher, T. 2006. Introduction to mathematical modeling of crop growth, p51-69. BrownWalker Press Boca Raton.

Goudriaan, J., and H.H. van Laar. 1978. Calculation of daily totals of the gross $CO_2$ assimilation of leaf canopies. Netherlands Journal of Agricultural Sciences 26:373-382.

Gourdriaan, J. and J.L. Monteith. 1990. A mathematical function for crop growth based on light interception and light interception and leaf area expansion. Ann. Bot. 66:695-701.

Heuvelink, E. 1999. Evaluation of a dynamic simulation model for tomato crop growth a development. Ann. Bot. 83:413-422.

Kuroyanagi, T.K. Yasuba, T. Higahide, Y. Iwasaki, and M. Takaichi. 2014.

Efficiency of carbon dioxide enrichment in an unventilated greenhouse. Biosys.Eng. 119:58-68.

Marcelis, L.F.M., E. Heuvelink, and J. Goudriaan. 1998. Modelling biomass production and yield of horticultural crops: a review. Sci. Hort. 74:83-111.

SAS. 2010. SAS 9.1 User's Guide. SAS Institute Inc., North Carolina, USA.

Tesi R., G. Chisci, A. Nencini, and R. Tallarico. 1995. Growth response to fertilization of sweet basil (*Ocimum basilicum* L.). Acta Hort. 390:93-96.

Thornley, J.H.M. 1977. Growth maintenance and respiration: a re-interpretation Ann. Bot. 41:1191-1203.

Thornley, J. H.M. and I.R. Johson. 2000. Plant and crop modelling, p 243-263. The Blackburn Press, NJ, USA

Yeo, K.H. and Y.B. Lee. 2004. The effect of $NO_3^-$-N and $NH_4^+$-N ratio in the nutrient solution on growth and 1uality of sweet basil. Kor. J. Hort. Sci. Technol. 22:37-42.

# CONCLUSION

In this study, photosynthesis and growth models of sweet basil and ice plant were developed for plant factory production. Particularly, biochemical models coupled with stomatal conductance and transpiration were considered for developing more accurate photosynthesis models. Saturation and compensation points of both plants for light and $CO_2$ were determined with the modified non-rectangular hyperbola model by regression analyses of light and $CO_2$ response curves, respectively. The maximum carboxylation rates, potential rates of electron transport, and rates of triose phosphate utilization for both plants were calculated by using Sharkey's regression. The results showed that the coupled biochemical model was effective for predicting the photosynthesis of both plants. The growth models of both plants for temperature and $CO_2$ concentration were developed by using expo-linear model.

Adequate air temperature and $CO_2$ concentration for both plants were suggested by experiments and growth models developed. From this study, we confirmed that the coupled biochemical models and the expo-linear models were more effective for explaining the photosynthesis and plant growth of both plants during the juvenile stage like plant factory conditions.

## ABSTRACT IN KOREAN

본 논문은 식물공장에서 바질과 아이스플랜트 광합성 모델과 생육 모델 개발에 연구이다. 특히 정교한 광합성 모델을 개발하기 위해 생화학적 모델에 기공전도도 및 증산 모델이 결합되었다. 바질과 아이스플랜트의 광과 탄산가스의 포화점과 보상점은 수정된 직각쌍곡선 모델에 의해 각각 구하였다. 광합성 생화학적 모델에 필요한 최대 카르복실화 속도와 3 탄당인산 이용 효율 및 전자전달의 속도는 Sharkey 의 방법에 의해 구하였다. 바질과 아이스 플랜트의 광합성을 예측하는데 회귀 모델과 비교하여 결합된 생화학 모델이 유효하다는 결과를 보여 주었다. 바질과 아이스 플랜트의 생육 모델은 선형 지수 모델을 이용해 온도와 탄산가스 농도에 관한 생육 모델을 개발하였다. 실험을 통해 적합한 온도와 탄산가스 농도가 제시되었고, 생육 실험에

기반하여 생육 모델이 개발되었다. 본 연구를 통해 식물공장에서 결합된 생화학적 광합성 모델과 선형 지수 모델에 기초한 생육 모델이 바질과 아이스플랜트의 광합성과 생육을 설명하는데 유효함을 확인하였다.

주요어: 광합성 모델, 생육 모델, 스위트바질, 아이스플랜트, 생화학적 모델

학번: 2003-30360